

DEVELOPMENT OF A NON-PINNED LOW-PROFILE END TREATMENT

A Thesis

by

FELICIA JEAN DESORCIE

Submitted to the Office of Graduate and Professional Studies of
Texas A&M University
in partial fulfillment of the requirements for the degree of

MASTER OF SCIENCE

Chair of Committee,	W. Lynn Beason
Committee Members,	C. Eugene Buth
	Dara W. Childs
Head of Department,	Robin Autenrieth

December 2013

Major Subject: Civil Engineering

Copyright 2013 Felicia Jean Desorcie

ABSTRACT

In the early 1990s, the Low-Profile Portable Concrete Barrier (PCB) system, including both the sloped Low-Profile PCB segment and Low-Profile PCB end treatment, were developed. The original Low-Profile PCB end treatment was designed with steel pins inserted along the barrier centerline, through precast holes, and anchored to the pavement or subgrade. The purpose of these pins was to reduce lateral deflection of the end treatment during an impact. For various reasons, users of the Low-Profile PCB system have stated that the system would be more easily deployed if the vertical pins were not used in situations where lateral deflections can be permitted. The primary objective of the research presented herein was to determine the feasibility of removing the vertical, steel pins from the Low-Profile PCB end treatment in certain applications and if necessary make modifications. The secondary objective of the research presented herein was to demonstrate the applicability of the finite element analysis (FEA) to unpinned barrier systems.

The research objectives were achieved through the use of sound engineering judgment, FEA, and a full-scale crash test. Based on sound engineering judgment and approximate strength analyses of the original Low-Profile PCB design, the author determined the system would most likely function acceptably but would have large lateral deflections. In order to increase connection rigidity and thus control lateral displacement, a plate washer was added to the barrier connection.

The modified non-pinned Low-Profile PCB system was tested for strength in a full-scale crash test under Manual for Assessing Safety Hardware (MASH) test 2-35. Additionally, the recommended system was analyzed under similar test conditions with LS-DYNA, a finite element code. The recommended system passed the MASH test 2-35, in both a full-scale crash test and FEA. While this does not replace the original barrier, it does provide another option for use of the Low-Profile PCB in situations where sufficient room for deflection outside of the length of need exists. If this room does not exist, the barrier must remain pinned.

DEDICATION

This thesis is dedicated to my parents, George and Caroline Desorcie, for their continuous love and support.

ACKNOWLEDGEMENTS

I would like to thank my committee chair, Dr. W. Lynn Beason, and my committee members, Dr. C. Eugene Buth and Dr. Dara W. Childs, for their guidance and support throughout the course of this research. Additionally, I would like to thank Dr. Akram Abu-Odeh and Michael Brackin for their support, especially with finite element analysis.

Thanks also to my friends and colleagues for making my time at Texas A&M University a fulfilling experience.

NOMENCLATURE

ASI	Acceleration Severity Index
FE	Finite Element
FEA	Finite Element Analysis
ft/s	Feet per Second
G	Gravitational Force
MASH	Manual for Assessing Safety Hardware
mi/h	Miles Per Hour
NCHRP	National Cooperative Highway Research Program
PCB	Portable Concrete Barrier
pcf	Pounds per Cubic Foot
PHD	Post-Impact Head Decelerations
TL-2	Test Level 2
THIV	Theoretical Head Impact Velocity
TTI	Texas A&M Transportation Institute

TABLE OF CONTENTS

	Page
ABSTRACT.....	ii
DEDICATION.....	iii
ACKNOWLEDGEMENTS.....	iv
NOMENCLATURE.....	v
TABLE OF CONTENTS.....	vi
LIST OF FIGURES.....	viii
LIST OF TABLES.....	x
CHAPTER I INTRODUCTION.....	1
CHAPTER II PROBLEM STATEMENT.....	4
CHAPTER III LITERATURE REVIEW.....	6
Concrete Barriers.....	6
Testing Methods.....	7
Full-Scale Crash Testing.....	7
Finite Element Analysis.....	8
Previous Research.....	10
Development of a Low-Profile Portable Concrete Barrier.....	10
Development of an End Treatment for a Low-Profile Concrete Barrier.....	12
Compliance Testing of an End Treatment for the Low-Profile Concrete Barrier.....	13
CHAPTER IV REVIEW, MODIFICATION, AND TESTING OF SYSTEM.....	15
Review of System.....	15
Slight Modifications to System.....	17
Low-Profile PCB System Design.....	19
Testing and Evaluation Criteria.....	22
CHAPTER V FINITE ELEMENT ANALYSIS.....	25
Design of Model.....	25

FE Results.....	28
Energy Values.....	28
Occupant Risk and Vehicle Stability.....	30
Summary.....	30
CHAPTER VI FULL-SCALE CRASH TESTING.....	32
Test Results.....	35
Occupant Risk and Vehicle Stability.....	42
Summary.....	42
CHAPTER VII FEA AND FULL-SCALE TESTING COMPARISON.....	45
CHAPTER VIII CONCLUSION.....	55
REFERENCES.....	56
APPENDIX A: LOW-PROFILE PORTABLE CONCRETE BARRIER DETAILS...	58
APPENDIX B: FINITE ELEMENT ANALYSIS ANGULAR DISPLACEMENT DATA.....	61
APPENDIX C: FULL-SCALE CRASH TEST INFORMATION	63

LIST OF FIGURES

	Page
Figure 2.1 Low-Profile PCB End Treatment Geometry.....	5
Figure 3.1 Low-Profile PCB Cross Section Comparison.....	11
Figure 4.1 Low-Profile PCB Connection Detail.....	16
Figure 4.2 Low-Profile PCB Connection Loading.....	16
Figure 4.3 Details of the Plate Washer.....	18
Figure 4.4 Typical Connection with Plate Washer.....	18
Figure 4.5 Layout of the Non-Pinned Low-Profile PCB Installation.....	20
Figure 4.6 Non-Pinned Low-Profile End Treatment before Test.....	21
Figure 4.7 Roll, Pitch, and Yaw Crash Test Sign Convention.....	24
Figure 5.1 Four-Node Shell Element.....	26
Figure 5.2 Eight-Node Solid Brick Element.....	26
Figure 5.3 FE Model Connection Detail.....	27
Figure 5.4 Contact Surfaces on Connection Between Barriers.....	28
Figure 5.5 Energy Distribution Time History.....	29
Figure 5.6 Summary of Results for FEA Simulation.....	31
Figure 6.1 Vehicle/Installation Geometrics.....	33
Figure 6.2 Vehicle Before Test.....	34
Figure 6.3 Installation and Vehicle Position After Test.....	35
Figure 6.4 Crash Test Summary Schematic.....	36
Figure 6.5 Installation After Test.....	38
Figure 6.6 Joint 2-3 Plate Washer Deformation.....	39

Figure 6.7	Vehicle After Test.....	40
Figure 6.8	Interior of the Vehicle Before and After Test.....	41
Figure 6.9	Summary of Results for Full-Scale MASH Test 2-35.....	44
Figure 7.1	Vehicle Angular Displacement Comparison.....	52
Figure A1	Low-Profile PCB Segment Details.....	59
Figure A2	Low-Profile PCB End Treatment Details.....	60
Figure B1	Vehicle Angular Displacements.....	62
Figure C1	Sequential Photographs (Overhead and Right Angle Views).....	68
Figure C2	Sequential Photographs (RearView).....	70
Figure C3	Vehicle Angular Displacements.....	71
Figure C4	Vehicle Longitudinal Accelerometer Trace.....	72
Figure C5	Vehicle Lateral Accelerometer Trace.....	73
Figure C6	Vehicle Vertical Accelerometer Trace.....	74

LIST OF TABLES

	Page
Table 7.1 Overhead View Sequential Comparison.....	46
Table 7.2 Right Angle View Sequential Comparison.....	48
Table 7.3 Rear View Sequential Comparison.....	50
Table 7.4 Occupant Risk Factor Comparison.....	52
Table 7.5 Yaw, Pitch, and Roll Maximum Value Comparison.....	53
Table C1 Vehicle Properties.....	64
Table C2 Measurement of Vehicle CG.....	65
Table C3 Exterior Crush Measurements.....	66
Table C4 Occupant Compartment Measurements.....	67

CHAPTER I

INTRODUCTION

Concrete barriers have been containing errant vehicles since the 1940s. These barriers typically serve one of two purposes; either to prevent vehicles from crossing over medians into opposing traffic, or to prevent errant vehicles from traveling into work zones. Throughout the years, barriers have been developed into two general categories: portable and permanent. The portable concrete barrier (PCB) is beneficial for use in work zones where the barrier can be easily deployed, while permanent concrete barriers are well suited for use in medians.

In the late 1980s to early 1990s, researchers at the Texas Transportation Institute (TTI) noticed that PCBs worked well for vehicles traveling through work zones, but they were creating a sight-distance problem. Specifically, this was a problem where there were openings in the longitudinal PCB allowing cross-traffic access. Thus, cross-traffic had to pull out into mainstream traffic before making eye contact with mainstream vehicles. This was especially a problem at night.

In the early 1990s, the Low-Profile PCB system, including both the Low-Profile PCB segment and sloped Low-Profile PCB end treatment, were developed (Guidry and Beason 1991). The main advantage of the Low-Profile PCB system is its height. The 20 inch height of the Low-Profile barrier system is significantly less than most other systems with typical heights of 32 inches or more. This system was an innovative approach to providing enhanced visibility to drivers in highway work zones or other appropriate locations in which cross-traffic access is required. The primary use of the barrier was in work zones at speeds of 45 mi/h or less. Thus, full-scale crash testing was completed ensuring that the entire Low-Profile PCB system would meet the necessary strength requirements for this type of barrier use.

The original Low-Profile PCB end treatment was designed with steel pins inserted every 24 inches, on the barrier centerline, through precast holes in the end treatment and anchored to the pavement or subgrade. The purpose of these pins was to

reduce lateral deflection of the end treatment during an impact when the barrier was deployed next to a vertical drop off. For various reasons, users of the Low-Profile PCB system have stated that the system would be more easily deployed if the vertical pins were not used in situations where lateral deflections can be permitted.

The primary objective of the research presented herein was to determine the feasibility of removing the vertical, steel pins from the Low-Profile PCB end treatment in certain applications and if necessary make modifications. The secondary objective of the research presented herein was to demonstrate the applicability of the FEA to unpinned barrier systems. This was done through the use of sound engineering judgment, finite element analysis, and a full-scale crash test. The entire system was modeled under Manual for Assessing Safety Hardware (MASH) test number 2-35 using the finite element program LS-DYNA. The model was run with a Chevrolet Silverado developed by the National Crash Analysis Center (NCAC). For the full-scale crash test, a 5,016 lb pick-up truck impacted the barrier at a speed of 45.0 mi/h and 25.3 degree angle. This test designation was used to test the strength of the barrier system with a non-pinned Low-Profile PCB end treatment.

The next chapter of this thesis presents the problem statement. The problem statement describes the issues with using vertical steel pins to anchor the end treatment to the pavement or subgrade. Chapter III discusses the history and development of concrete barriers as a whole with an in depth view of the development of the Low-Profile portable concrete barrier. In addition, this chapter illustrates the significance of crash simulation in the development of barriers. Chapter IV describes the engineering review of the original Low-Profile PCB system with a non-pinned end treatment. This chapter also provides justifications for the modification that was made to the system prior to testing. Additionally, this chapter describes the Low-Profile PCB system, with a non-pinned end treatment, which was tested and simulated. Lastly, this chapter identifies the test criteria and evaluation for analysis of the system. Chapter V presents the development and results of the Finite Element model. Chapter VI depicts the full-scale crash test including before and after descriptions. Furthermore, the full-scale crash

test data are presented. Chapter VII compares the results from the Finite Element Analysis and the full-scale crash test. Moreover, this chapter discusses the similarities and differences between the results and provides reasoning for why the differences exist. Finally, Chapter VIII summarizes the results and draws conclusions on the research presented within.

CHAPTER II

PROBLEM STATEMENT

The Low-Profile Portable Concrete Barrier (PCB) system was initially developed in the early 1990s. The development of the system began with the innovative design of the Low-Profile PCB segment and continued with the engineering of the Low-Profile PCB end treatment. The sloped Low-Profile PCB end treatment was initially designed with a series of vertical pins, every 24 inches on center, inserted through precast holes in the end treatment and anchored to the pavement or subgrade. Figure 2.1 depicts the geometry of the Low-Profile PCB end treatment. These anchor pins were designed to reduce the lateral deflection of the end treatment during impact. The design was successful in controlling lateral deflection; however, this method introduced holes into the pavement or subgrade. Also, in some cases control of lateral deflection is not required.

The introduction of holes into pavement or subgrade contributes to decreased local integrity. The use of the steel pins also creates a greater barrier installation time. Thus, it was determined by users and engineers that the elimination of the steel pins would provide a more easily deployed barrier system in situations that permitted lateral deflections. Additionally, the removal of steel pins from the system would result in no holes being introduced into pavement or subgrade.

The original system will need to be reviewed without the use of the vertical pins in order to determine the feasibility of removing the vertical, steel pins from the Low-Profile PCB end treatment in certain applications and if necessary make modifications. The design shall allow for the extension of the National Cooperative Highway Research Program Report 350 strength certification to the non-pinned end treatment, which already exists for the current Low-Profile PCB system.

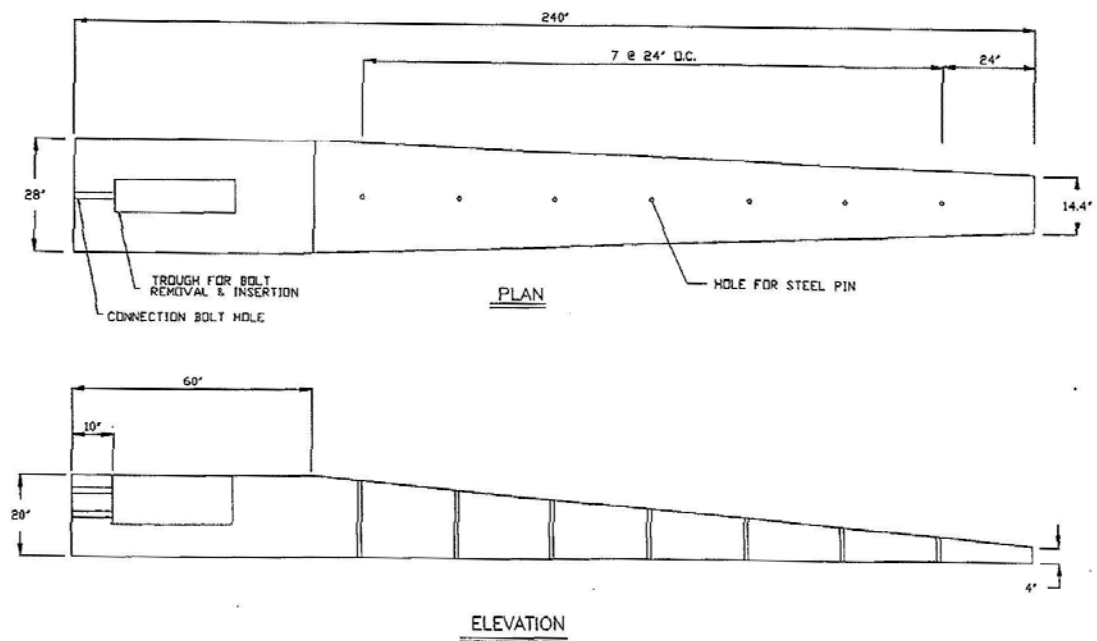


Figure 2.1: Low-Profile PCB End Treatment Geometry
(Guidry and Beason 1991)

CHAPTER III

LITERATURE REVIEW

This chapter focuses on the development of concrete barriers as a whole with an in depth view of the development of the low profile portable concrete barrier. Additionally, this chapter illustrates the importance of testing methods on the development of barriers including finite element simulation and full-scale crash testing.

CONCRETE BARRIERS

Concrete barriers are used to keep errant vehicles from traveling off the road or into opposing traffic. Most commonly, concrete barriers are used in medians to prevent vehicles from crossing over into opposing lanes of traffic and in work zones which create a hazardous environment for both workers and motorists. There are two different types of concrete barriers, those utilized as permanent barriers and those used as portable barriers. Portable Barriers provide an excellent form of safety for construction workers without investing too much time installing protection.

Concrete Barriers have developed over the years as a means to solving a problem. “This first generation of concrete barriers was developed to (a) minimize the number of out-of-control trucks penetrating the barrier, and (b) eliminate the need for costly and dangerous median barrier maintenance in high-accident locations with narrow medians” (Kozel 1997). Through the continued design and re-design of concrete barriers a variety of highly sophisticated shapes have been developed including the New Jersey Shape, General Motors Shape, F-Shape, Single Slope Shape and Low-Profile Shape. Each shape uses different heights, angles, and slope lengths to provide a concrete barrier that “fills a niche and helps meet the needs of highway agencies that select, design, and locate traffic barriers” (McDevitt 2000).

Portable Concrete Barriers (PCBs), which are primarily used in the construction industry of transportation, are a series of safety shape sections that are connected creating a continuous longitudinal barrier (McDevitt 2000). Since these devices are primarily used in work zones where hazardous environments are close to the flow of

traffic, it is important to keep lateral deflections to a minimum. Minimizing lateral deflections can be done in an assortment of ways including, but not limited to, increasing the moment capacity of the joints within the entire barrier and placing steel pins in the barrier to act as an anchor. “Anchoring each barrier segment with steel pins driven into the ground is very effective, but it is labor-intensive and makes the barrier less portable” (McDevitt 2000).

While the shape of the barrier is important, it is of equal significance to note the variety of end treatments that can be applied to different barriers. Just as each concrete barrier fills a niche, different end treatments are intended for various situations. Although the end treatment is placed outside the length-of-need, it will still have an effect on how the barrier will respond if the errant vehicle were to strike the end treatment instead of the barrier.

TESTING METHODS

A variety of developments have been made over the years since the original development of the New Jersey Concrete Median Barrier, which was designed through the use of observations on operational problems while the barrier was in use. Now, roadside safety apparatuses can be tested through either full-scale crash testing or finite element simulation. These methods provide researchers with the ability to ensure that a device is crashworthy before installing the device on the roadway.

Full-Scale Crash Testing

A full-scale crash test is a form of destructive testing that is conducted to not only test the ability of a device to perform the intended job but to also test the occupant safety. The first set of full-scale crash testing procedures were developed for testing guardrails and published in 1962 in the Transportation Research Board (TRB) *Highway Research Correlation Services Circular 482*. The document continued to develop with a publication in 1974 of the *National Cooperative Highway Research Program (NCHRP) Report 153: Recommended Procedures for Vehicle Crash Testing of Highway Appurtenances*. This document was published to address questions that had come about from the original publication in 1962. Shortly after the development of NCHRP Report

153, *Transportation Research Circular* 191 was published to address particular issues with NCHRP Report 153. As more testing began to take place, there were more questions to be answered about the testing methods. Thus, another document was published in 1980 to answer these questions titled *NCHRP Report 230: Recommended Procedures for the Safety Performance Evaluation of Highway Safety Appurtenances* (Michie 1980). This document included an updated evaluation criterion and brought documentation up to speed with the technology at the time. In 1993, *NCHRP 350: Recommended Procedures for the Safety Performance Evaluation of Highway Features* was developed to address significant changes to vehicles, the development of new barriers, and additional technological advances becoming prevalent (Ross et al 1993).

The American Association of State Highway and Transportation Officials (AASHTO) *Manual for Assessing Safety Hardware* (MASH) is the current publication that sets the guidelines and standards for evaluating the crashworthiness of roadside safety devices through full-scale crash testing (AASHTO 2009). This document supersedes *NCHRP Report 350*. MASH provides a set of guidelines which creates a uniform way to test and evaluate roadside safety devices. The goal of these guidelines is to test the “worst practical conditions” for which the test article may receive during installation. Thus, it is this philosophy which shall be used when selecting vehicle size, speed, angle of impact, etc. The MASH framework is equal to or more severe than *NCHRP Report 350*.

Finite Element Analysis

Finite Element Analysis (FEA) utilizes mathematical models to simulate scientific physical interactions. The National Science Foundation (NSF) defines simulation as the application of computational models to the study and prediction of physical events or the behavior of engineered systems. In 2006, NSF developed a report titled “Simulation-Based Engineering Science” with the objective of exploring opportunities for and potential advance in simulation-based engineering science (SBES). In this report NSF stated: “With the depth of its intellectual development and its wide range of applications, computer simulation has emerged as a powerful tool, one that

promises to revolutionize the way engineering and science are conducted in the twenty-first century” (Oden et al 2006). While FEA has been used for more than a half century, it has been within the past decade that the application of FEA has been utilized more accurately in industrial applications. The report identified that there have been successful simulations in crashworthiness studies but that simulation in industry has not yet met its full potential. This is due to a variety of limitations such as the complexity of model design, lack of methods to link models of varying scales, and the separation of design optimization and FEA. With particular attention to roadside safety devices, it is the complexity of the model and the need for validation with a full-scale crash test that finds this technology limited and being mostly utilized in the last stages of design.

While limitations do exist, the power of being able to use FEA to develop and enhance the design of devices has been the driving force for improving the capabilities of FEA programs. However, “nonlinear physical behavior is extremely complicated, and capturing that behavior with mathematics is not an exact science” (Reid 2004).” Engineers and researchers must be creative in the modeling of the system being tested. “Parts that do not deform significantly can be made rigid, and parts that undergo nonlinear, large deformations must be modeled with elastic-plastic constitutive models” (Marzougui 2001). Thus, in connection to a concrete median barrier, the barrier itself would be rigid and all connections would be modeled as elastic-plastic pieces.

In addition, it has been determined that there are a few significant aspects of barriers that must be modeled with care in order to yield simulation results which are consistent with full-scale crash tests. Ensuring the shape, slope, connections, and friction are modeled with high precision will result in an accurate model of the system. The mass and inertial properties are determined by the shape, which will affect the overall deflection and displacement of the barrier. The slope of the barrier helps in determining the vehicles post-impact trajectory including roll, pitch, and yaw, as well as, whether or not the vehicle will ramp up the barrier. The connection between barriers is typically steel which is likely to deform under an impact from a vehicle. The connection also plays an intricate role in the barrier’s ability to withstand deflections, which requires

extreme attention to the complexity of the design while modeling in a FEA modeling program. The last noteworthy issue influencing the model is the friction between the barrier and the surface on which the barrier rests. This will likely require friction testing before modeling. If modeled with incorrect friction factors, the barrier is likely to deflect more or less than it would in reality.

Simulation is a very powerful tool which must be treated with attention and diligence. The shape, slope, connection, and frictional attributes of a barrier system require the most attention. Once the barrier is modeled, the model needs to be compared with a full-scale crash test in order to be able to quantify the reliability of the FEA results. Minor adjustments can then be made to the barrier system and the FEA shall be a good measure of how the new system would behave under real world conditions.

PREVIOUS RESEARCH

There is a significant amount of previous research on concrete barriers, however for the purposes of this document this section will focus on previous research and development of the Low-Profile barrier.

Development of a Low-Profile Portable Concrete Barrier

The Low-Profile Portable Concrete Barrier was originally developed by researchers at the Texas Transportation Institute (TTI) in the early 1990s (Guidry and Beason 1991). The objective of the barrier was to shield errant vehicles from hazards introduced by work zones while improving visibility. It was determined that visibility was an issue, particularly in areas where cross-traffic access is required such as parking lots and intersecting roads. Therefore, with a height of 20 inches, the Low-Profile barrier provides a significant visibility advantage to drivers over most other standard barrier systems with a typical height of 32 inches. Figure 3.1 illustrates the significant difference in shape between the Low-Profile PCB (solid line) and the New Jersey Shape (dashed line), which can be taken as a conventional shape. The height of the barrier was designed from sight distance analysis which included evaluation of headlight height, eye height of the driver, and roadway geometry requirements.

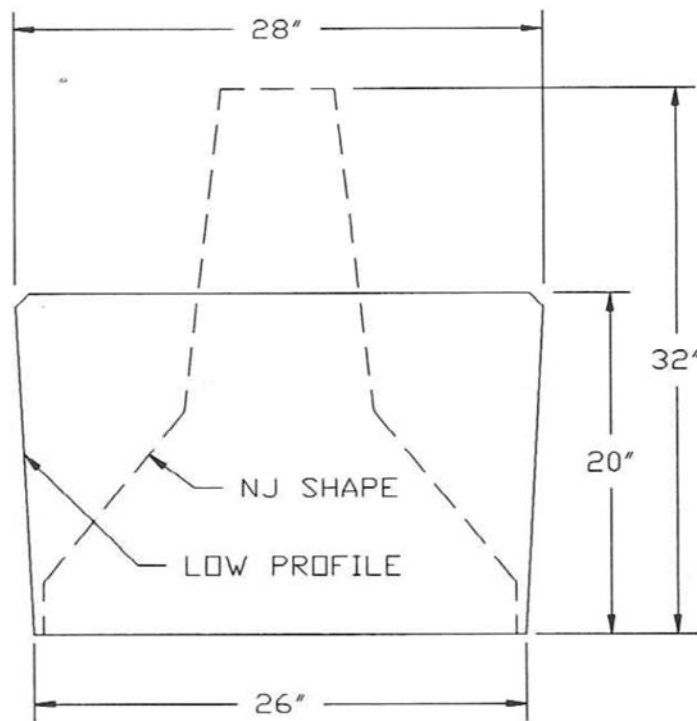


Figure 3.1: Low-Profile PCB Cross Section Comparison
(Guidry and Beason 1991)

The Low-Profile barrier was designed with a negative 1:20 vertical slope which reduces the vertical displacement of the vehicle on the impact side. The system is designed with 20-foot Low-Profile segments allowing the system to tolerate both vertical and horizontal roadway curves, within 4 degrees, while still maintaining a barrier weight that reduces lateral deflections. The unique connection developed for the Low-Profile barrier system aides in reducing lateral deflections by having a moment capacity greater than 100,000 ft-lbs. “The connection is accomplished by aligning the ends of two barrier segments and inserting two ASTM A36 bolts through the connection holes which are recessed into a rectangular trough which is cast into the end of each segment” (Guidry and Beason 1991).

The barrier system was tested in compliance with NCHRP Report 230. A test of strength and a test of vehicle stability were conducted on this system. Since the system was intended to be used in urban work zones, where the maximum speed was 45 mi/h,

the system was tested at an impact speed of 45 mi/h. For the test of strength, a ¾ ton pick-up truck impacted the barrier at a speed of 45 mi/h and 25-degree angle. For the test of stability, a 1,800 lb small car impacted the barrier at a speed of 45 mi/h and a 20-degree angle. The researchers and engineers believed that these two test conditions were representative of the most reasonably, severe impact for this application. The tests demonstrated that the barrier system could endure such impacts without any substantial damage to the barrier and without excessive rolling or vaulting of the vehicle.

Development of an End Treatment for a Low-Profile Portable Concrete Barrier

In order for the Low-Profile PCB to be used, it was necessary for engineers to develop a suitable end treatment. A variety of end treatments exist and they fall into one of three categories: blunt end, sloped end, or energy-absorbing end. With the 20-inch height being a unique advantage to the Low-Profile barrier, it was impossible for engineers to simply apply a current end treatment to this distinctive barrier as all other end treatments were designed for barriers with heights of 32 inches. Therefore, engineers needed to develop a new barrier style or modify existing styles.

While all end treatments have advantages and disadvantages, it was the major disadvantages that set the different styles apart from one another. Blunt end treatments were likely to cause extreme vehicular accelerations if an end-on impact occurred. Thus, the only way to use this style of end treatment would require a flared end making an end-on impact nearly impossible. Sloped end treatments were likely to cause an errant vehicle to be rolled or launched. However, if engineers were to keep with the 1:20 negative slope of the Low-Profile PCB, the errant vehicle would have reduced vertical accelerations resulting in less chance for a vehicle to launch or roll. The energy-absorbing end treatment has a significant advantage over other end treatments with its ability to bring a vehicle to a controlled stop. Unfortunately, energy-absorbing end treatments are more expensive.

With the knowledge of different end treatment styles, engineers decided to focus on a need for an end treatment that was 20 inches or less in height, had the same redirective qualities as the original barrier, and was affordable. With that in mind, it

was the decision of the engineers to use a longitudinally sloped end treatment. Thus, the first 5 feet of the end treatment were kept at a height of 20 inches to allow for the uniform connection between barriers and then the barrier was sloped linearly to a height of 4 inches at the impact end. Additionally, this design kept the same negative 1:20 vertical slope and connection as the barrier segments. To reduce lateral deflections, steel pins were inserted every 24 inches through precast holes in the end treatment to the pavement, acting as anchors.

The constant slope Low-Profile end treatment was tested in compliance with NCHRP Report 230 (Beason 1992). The end treatment was attached to four segments and tested three times. Since the system was intended to be used in urban work zones, where the maximum speed was 45 mi/h, the system was tested at an impact speed of 45 mi/h. For the first test, a 1,800 lb small car impacted the end treatment 6.5 feet from the end with an angle of 15 degrees. For the second test, a 1,800 lb small car impacted the end treatment end-on, with the centerline of the right wheel lined up with the centerline of the end treatment. For the third test, a ¾ ton pick-up truck impacted the end treatment end-on, with the centerline of the vehicle lined up with the centerline of the end treatment. The researchers and engineers believed that these three test conditions were representative of the most severe impact for this application. The tests demonstrated that the end treatment could endure such impacts without any substantial damage to the barrier and without excessive rolling or vaulting of the vehicle.

Compliance Testing of an End Treatment for a Low-Profile Portable Concrete Barrier

Soon after the development of the Low-Profile barrier and the Low-Profile end treatment, NCHRP Report 350 superseded NCHRP Report 230. Through evaluation of the Low-Profile barrier test result, engineers determined that the testing conducted under NCHRP Report 230 met the level 2 NCHRP Report 350 crash test criteria. However, after evaluation of the Low-Profile end treatment test results, engineers determined that new tests needed to be conducted in order to meet level 2 NCHRP Report 350 crash test criteria. Under NCHRP Report 350 the Low-Profile end treatment is considered a gating

terminal. Thus, seven different crash testing conditions must be met in order to fulfill test level 2 crash criteria. These various conditions were tested, and TTI researchers found the Low-Profile end treatment to comply with NCHRP Report 350 test level 2 criteria (Beason et al 1998).

CHAPTER IV

REVIEW, MODIFICATION, AND TESTING OF SYSTEM

This chapter provides a review of the original Low-Profile Portable Concrete Barrier (PCB) system with a non-pinned end treatment. A description of the slight modification made to the connection is explained. Additionally, this chapter provides a description of the Low-Profile PCB system, with a non-pinned end treatment, that was tested and simulated. Lastly, this chapter identifies the conditions under which the article was tested and evaluated in both a Finite Element Analysis and full-scale crash test.

REVIEW OF SYSTEM

With the removal of the steel pins from the end treatment of the Low-Profile PCB, the system needed to be evaluated with sound engineering judgment and simplified calculations. The original assessment analyzed the original system with the removal of the vertical steel pins only. The analysis illustrated significant rotation about the connection between the end treatment and the first barrier segment, producing lateral deflections. Thus, the author believed the system was likely to work; however, the lateral displacement of the system would prevent such a barrier from being deployed next to a drop off. Without steel pins, the lateral deflection of the Low-Profile end treatment can only be controlled by the following: rigidity of the connection, mass of the end treatment, and frictional forces between the end treatment and the supporting surface. It was the author's opinion to focus on the rigidity of the connection in order to avoid any major redesigning of the Low-Profile PCB system.

The original connection between the barriers in the Low-Profile PCB system was accomplished by inserting two, ASTM A36, 1 ¼ inch threaded steel rods through two precast holes in the connecting barrier ends. Figure 4.1 illustrates the connection detail. The design specifications for the Low-Profile PCB system state that these threaded steel rods shall be secured with standard SAE J995 Grade 5 washers and nuts. This type of connection allows the threaded steel rods to carry a centric tensile force which is coupled

with a compression stress carried by the concrete as the barrier faces come in contact. This creates a moment resisting connection. Figure 4.2 illustrates the connection loading.

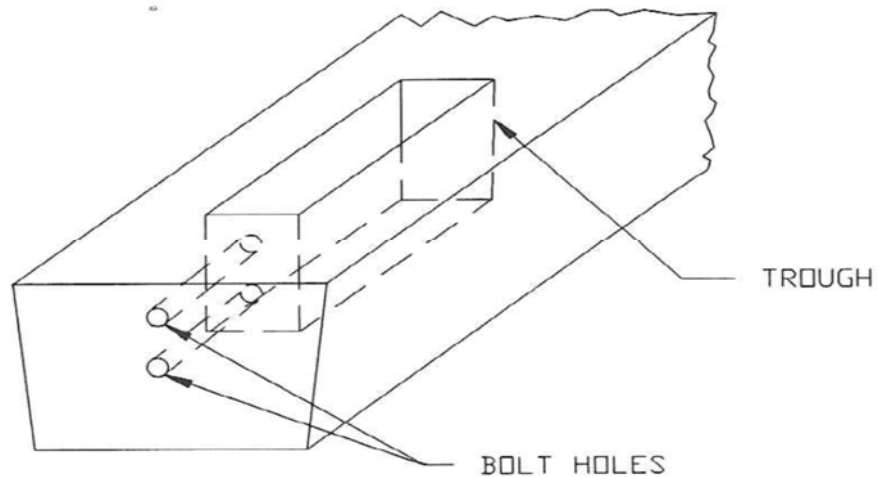


Figure 4.1: Low-Profile PCB Connection Detail
(Guidry and Beason 1991)

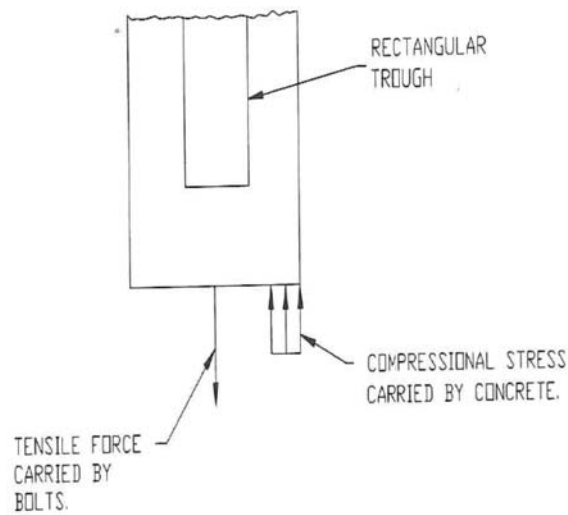


Figure 4.2: Low-Profile PCB Connection Loading
(Guidry and Beason 1991)

SLIGHT MODIFICATIONS TO SYSTEM

Approximate strength analyses were conducted on the Low-Profile PCB system with the non-pinned Low-Profile PCB end treatment, with a focus, on the rigidity of the connection. With significant rotation being induced on the connection when vertical steel pins are not used, it is necessary to increase the stiffness of the connection in order to counteract the increased rotational force. Thus, it is essential that the threaded steel rods develop their tensile forces, which then transfers to the barrier face by the nuts and washers. The author believed that the standard washer was not sufficient transfer the force from the nuts to the concrete barrier. Thus, it was the opinion of the author to add a 5 x 10 x 3/8 inch, ASTM A36 steel plate washer insuring the connection threaded steel rod would be able to reach its full potential. The plate washer was cut out of flat strap and contains two symmetrically placed holes, allowing the plate washer to slip over both ends of the threaded steel connection rods. The standard washer is then placed between the plate washer and standard nut. The plate washer is to be used on both sides of the connection. Figure 4.3 depicts the new plate washer. Figure 4.4 shows a typical connection with the use of the plate washer.

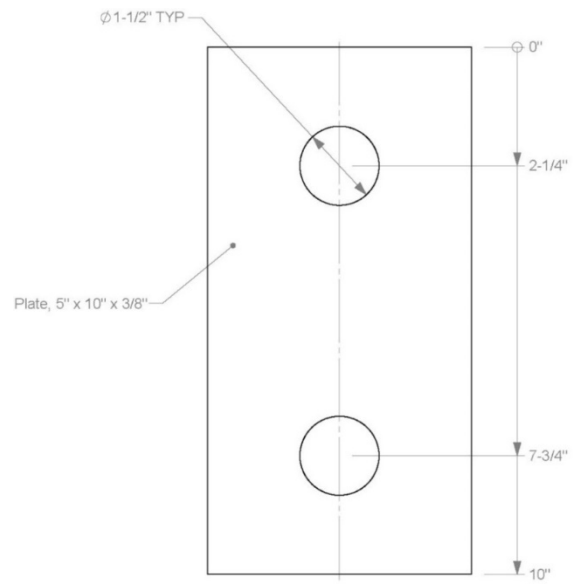


Figure 4.3: Details of the Plate Washer



Figure 4.4: Typical Connection with Plate Washer
(Beason et al 2013)

LOW-PROFILE PCB SYSTEM DESIGN

The Low-Profile PCB end treatment and the Low-Profile PCB segments are constructed in lengths of 20 feet. Also, the connection end of the Low-Profile PCB end treatment and the Low-Profile PCB segments are at a height of 20 inches and contain the same connection. This connection, discussed above, consists of two, ASTM A36 1 ¼ inch threaded steel rods, two 5 x 10 x 3/8 inch, ASTM A36 steel plate washers, and four SAE J995 Grade 5 washers and nuts. The Low-Profile PCB end treatment maintains a height of 20 inches for 5 feet, along the length of the barrier, before sloping down to a height of 4 inches at the end of the Low-Profile PCB end treatment. Additionally, the Low-Profile PCB end treatment is tapered horizontally along the entire length of the barrier from 28 inches to 14.5 inches. The Low-Profile PCB is also tapered vertically along the impacting face with a negative slope of 1:20. Lastly, the Low-Profile PCB system contains appropriate reinforcing throughout. Construction drawings for both the Low-Profile PCB end treatment and Low-Profile PCB segment are provided in Appendix A.

The constructed Low-Profile PCB system consisted of six Low-Profile PCB segments and two non-pinned Low-Profile PCB end treatments. Connections were modified with the use of the plate washer as described above. Figure 4.5 presents details of the Low-Profile PCB system as it was constructed for testing. Figure 4.6 depicts the Low-Profile PCB system prior to testing.

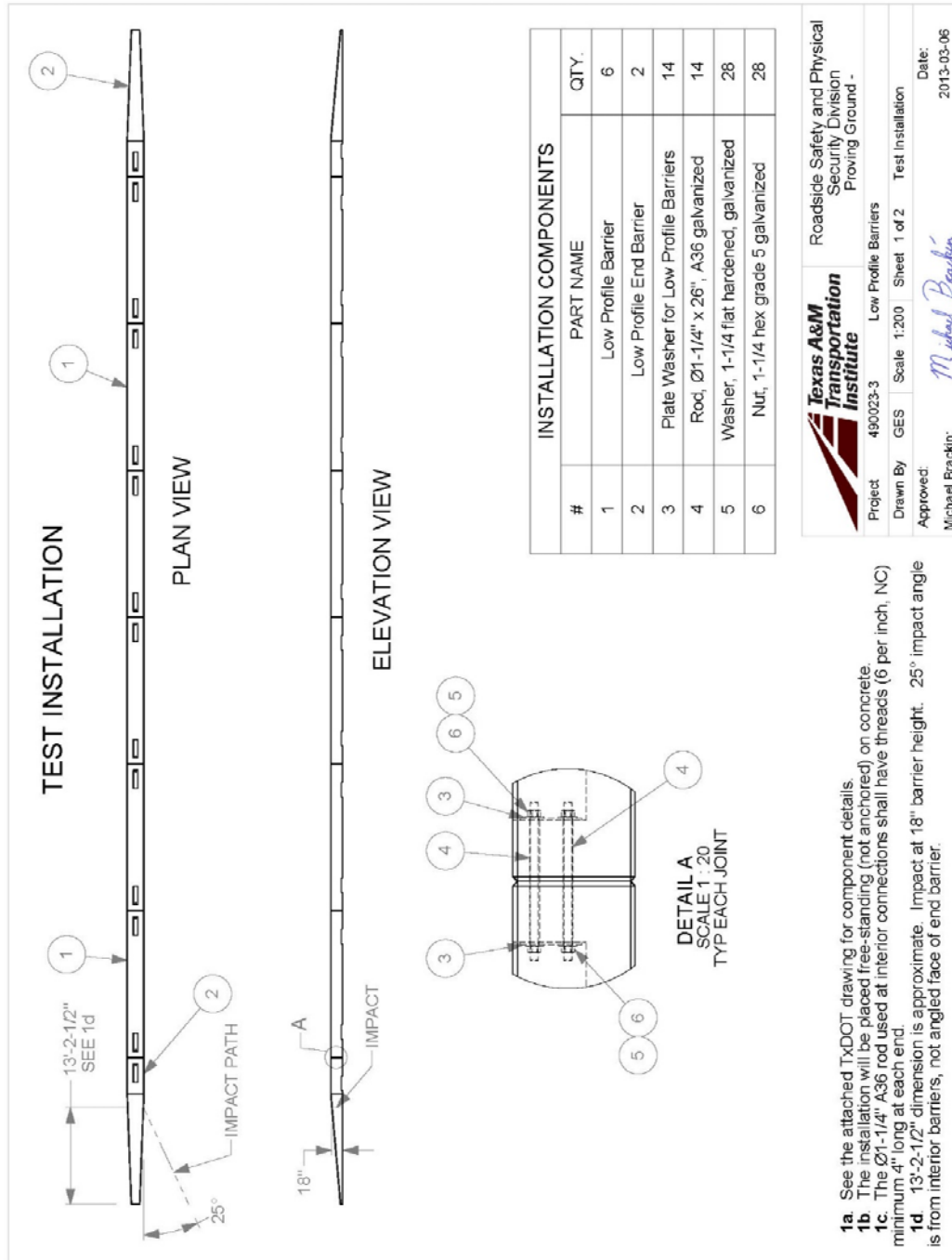


Figure 4.5: Layout of the Non-Pinned Low-Profile PCB Installation
(Beason et al 2013)



a) Impact Side



b) Field Side

Figure 4.6: Non-Pinned Low-Profile End Treatment Before Test
(Beason et al 2013)

TESTING AND EVALUATION CRITERIA

The Low-Profile PCB system had previously been certified to be in compliance with NCHRP Report 350 TL-2 requirements. Thus, it was the testing objective of the non-pinned Low-Profile PCB end treatment to extend the strength certification under the current testing standards of MASH. Certification requirements within MASH are equal to or more severe than NCHRP Report 350.

Of the tests involved in achieving re-certification, this research focuses on what the author believed to be the most severe strength test, MASH test 2-35. This test was selected to be the most severe strength test as it was the test that provided the greatest force (5,000 lb pickup truck) at the steepest approach angle (25 degrees). The last test criteria that needed to be decided upon was the critical impact location. If the full-size pickup impacted the Low-Profile PCB system at the joint between the non-pinned Low-Profile PCB end treatment and the first Low-Profile PCB segment, then there would be minimal difference whether or not the end treatment was pinned. The author determined there was some critical point between the connection end and the nose of the Low-Profile PCB end treatment where the pickup truck would begin to redirect. The point at which the barrier will redirect the truck and not act as a gating system is known as the beginning of length-of-need. This impact location would provide the greatest test of strength for the non-pinned Low-Profile PCB end treatment by applying the greatest moment to the connection between the end treatment and the PCB segment. It is at this critical point that the effects of the Low-Profile PCB end treatment not being pinned will be greatest. Through finite element analysis and engineering judgment, this point was determined to be at 13.2 feet from the nose of the end treatment. The formal description of the test that was conducted to extend the certification of the non-pinned Low-Profile PCB end treatment is as follows:

MASH test 2-35: A 2270P (5000-lb) pickup truck impacting the terminal at a nominal impact speed and angle of 44mi/h and 25 degrees, respectively, with the corner of the bumper aligned with the beginning of the length of need of the

terminal. The test is primarily intended to evaluate structural adequacy and vehicle trajectory criteria. (Beason et al 2013)

The system was evaluated for vehicle stability, occupant risk, and structural adequacy. Vehicle stability was assessed through vehicle angular velocities known as roll, pitch and yaw. Yaw, pitch, and roll describe the vehicles rigid body rotation about the x-axis, y-axis, and z-axis, respectively. Figure 4.7 displays yaw, pitch, and roll crash test sign convention. The axes are vehicle fixed and dependent upon being read in the following sequence: yaw, pitch, roll. Occupant risk estimates the potential risk of hazard to the vehicle occupants or those in the surrounding area. Occupant risk is appraised from the data collected by the accelerometer located at the center of gravity of the vehicle and deformation or intrusion into the occupant compartment. The acceleration data is analyzed and provides occupant impact velocity, ridedown acceleration, Acceleration Severity Index(ASI), Theoretical Head Impact Velocity(THIV), Post-Impact Head Decelerations(PHD). These calculations are assessing the response of a hypothetical, unrestrained front seat occupant who is likely to travel through space until contacting an interior surface. Occupant impact velocity and ridedown acceleration are describing the change in velocity the hypothetical occupant feels at impact and the acceleration from the collision just after impact. THIV is the magnitude of the change in velocity of the hypothetical occupant's head when it strikes the surface within the interior of the vehicle. PHD is the change in acceleration the hypothetical occupant's head would feel after impacting a surface within the interior of the vehicle. ASI provides a measure of the severity of the vehicular motion during impact for the hypothetical occupant. Lastly, the structural adequacy of the system is determined by the barrier's ability to contain and redirect the vehicle.

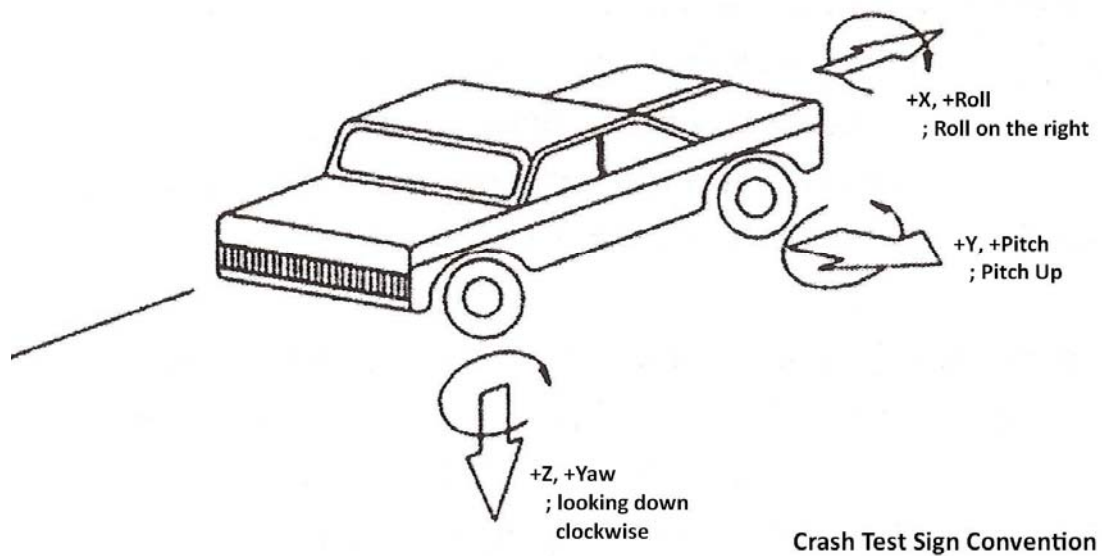


Figure 4.7: Roll, Pitch, and Yaw Crash Test Sign Convention

CHAPTER V

FINITE ELEMENT ANALYSIS

Recent advances in finite element (FE) methodologies have provided researchers in the roadside safety community the ability to investigate complex dynamic problems. The finite element analysis (FEA) discussed herein was generated using HyperMesh version 12.0 and analyzed using LS-DYNA finite element code (Hallquist 2012). LS-DYNA is widely used to solve nonlinear, dynamic responses to three-dimensional problems. This explicit FE code is capable of capturing complex interactions that occur when a vehicle impacts a barrier system, such as the Low-Profile Portable Concrete Barrier (PCB) system.

DESIGN OF MODEL

Two finite element (FE) models were used in computer simulations to predict structural capacity and occupant risk of the Low-Profile PCB system when impacted at 44 mi/h and 25 degrees with a MASH 2270P pickup truck. One model was of the Low-Profile PCB and the other of the truck. The FE model of the MASH 2270P pickup truck is a 2270 kg Chevrolet Silverado pickup truck developed by National Crash Analysis Center (NCAC). The FE model of the Low-Profile PCB system was developed per the design drawings to accurately replicate the geometry. Design drawings are presented in Appendix A.

The FE model of the Low-Profile PCB system consisted of seven different components: barrier segments, end treatments, threaded steel rods, plate washers, washers, nuts, and the ground. Figure 5.1 and 5.2 illustrate the two different types of elements, four-node shell elements and eight-node solid brick elements that were used throughout the model. The mesh density and aspect ratio selected for this analysis are consistent with criteria established at TTI Proving Grounds.

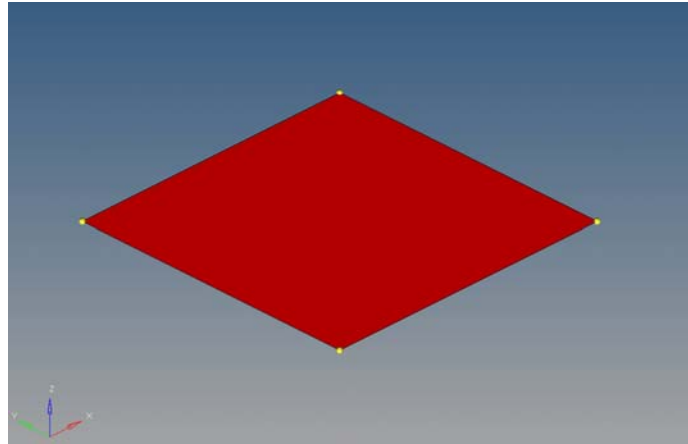


Figure 5.1: Four-Node Shell Element

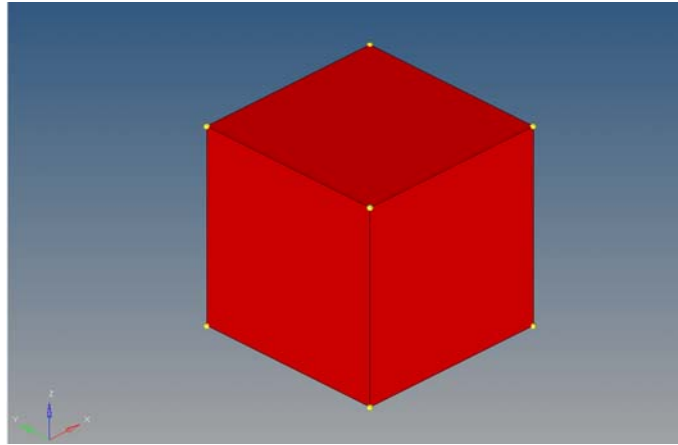


Figure 5.2: Eight-Node Solid Brick Element

The concrete section of both the barrier segments and end treatments were modeled using eight-node, rigid, solid brick elements. The density of the concrete was considered to be 150 pcf. “Approximating a deformable body as rigid is a preferred modeling technique in many real world applications” (Hallquist 2012). The threaded steel rods were modeled using eight-node, elastic, solid brick elements with a stress strain curve for A36 steel. The steel sections of the plate washers were modeled using four-node, elastic, shell elements with a stress strain curve for A36 steel. Similarly, the washers and nuts were modeled using four-node, elastic, shell elements with Grade 5

steel properties. Lastly, the concrete section of the ground was modeled using four-node, rigid, shell elements. Figure 5.3 illustrates the connection within the FE model.

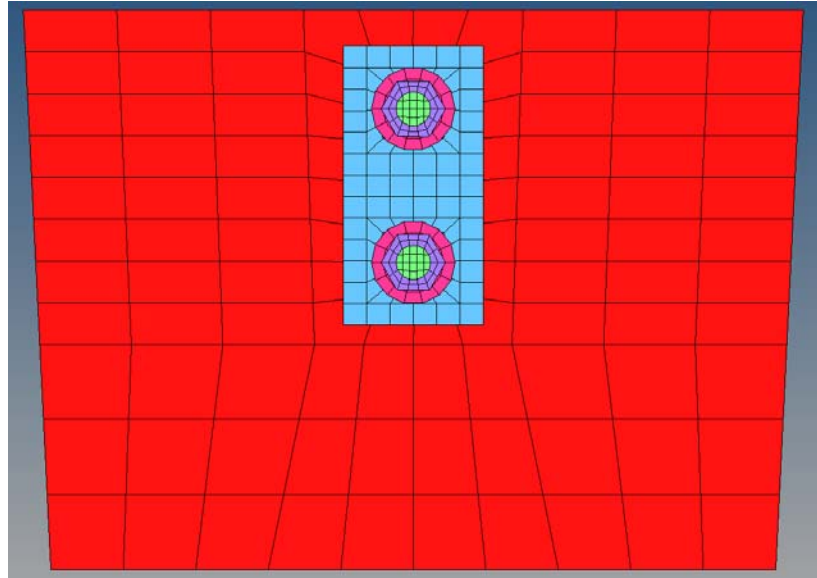


Figure 5.3: FE Model Connection Detail

A contact was placed between the nut and washer, washer and plate washer, washer and threaded steel rod, plate washer and barrier, and plate washer and threaded steel rod. Barriers contact one and other with an applied frictional coefficient of 0.45. A contact was defined between the threaded steel rods and the connection holes in the barrier. The static frictional coefficient between the ground and barriers is 0.63 while the dynamic frictional coefficient is 0.26. These values were selected based on testing conducted by NCAC in which they drag PCBs on concrete to determine frictional coefficients. Figure 5.4 illustrates the contacts, in dark blue, as they exist on the surface of the barrier, plate washer, and washer.

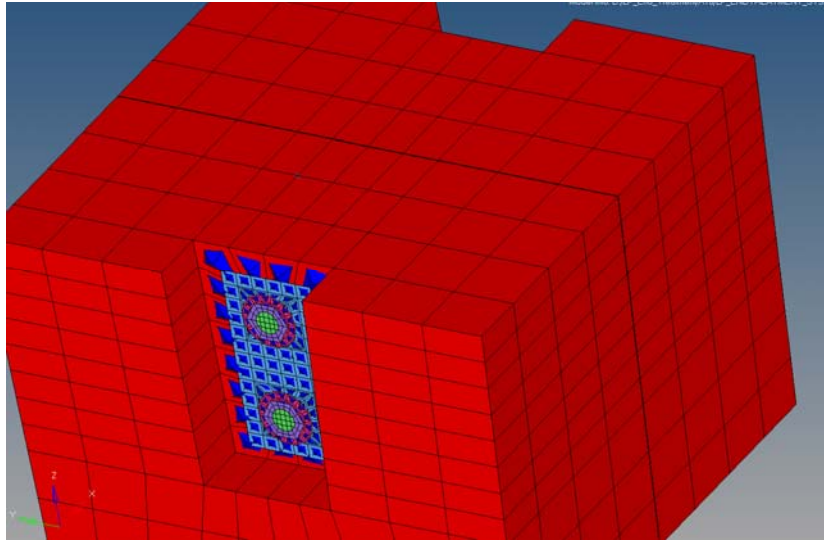


Figure 5.4: Contact Surfaces on Connection Between Barriers

FE RESULTS

The vehicle was traveling at a speed of 44.0 mi/h when it impacted the non-pinned Low-Profile end treatment 79 inches from joint between the end treatment and first barrier. The impact angle was 25 degrees. At approximately 0.01 s the vehicle made contact with the end treatment which began to deflect towards the field side, and at 0.06 s, the vehicle began to redirect. The vehicle was traveling parallel with the barrier at 0.335 s, and the rear of the vehicle contacted the barrier at 0.370 s. Maximum deflection of the barrier occurred at 0.710 s.

Energy Values

The kinetic energy applied to the barrier by the truck is reduced as it is converted into other forms of energy within the system. Internal energy is any energy stored in a component through deformation. Sliding interface energy is represented by the energy dissipated due to friction between components. Finally, hourglass energy is an unreal numerical energy dissipated by LS-DYNA. Figure 5.5, illustrates the conversion of kinetic energy into other forms of energy within the system as the simulation progresses in time.

Since this is a closed system, energy shall be conserved. Thus, the sum of the internal energy, kinetic energy, sliding interface energy, and hourglass energy should equate to the initial kinetic energy of the truck. Approximately 12 percent of the initial kinetic energy of the impacting truck is converted into internal energy. Approximately 21 percent of the initial kinetic energy is converted into sliding interface energy. Approximately 1 percent of the initial kinetic energy is converted into hourglass energy. Sixty four percent of the initial kinetic energy has yet to be dissipated by the truck at the time the truck leaves the barrier system. This is mainly due to the kinetic energy remaining in the truck as it exits the barrier with an exit velocity. The slight reduction in total energy of the system is due to numerical computation and loss of energy in the deformation of the barrier and connections. This is not of great concern as less than 6 percent of the total energy is lost.

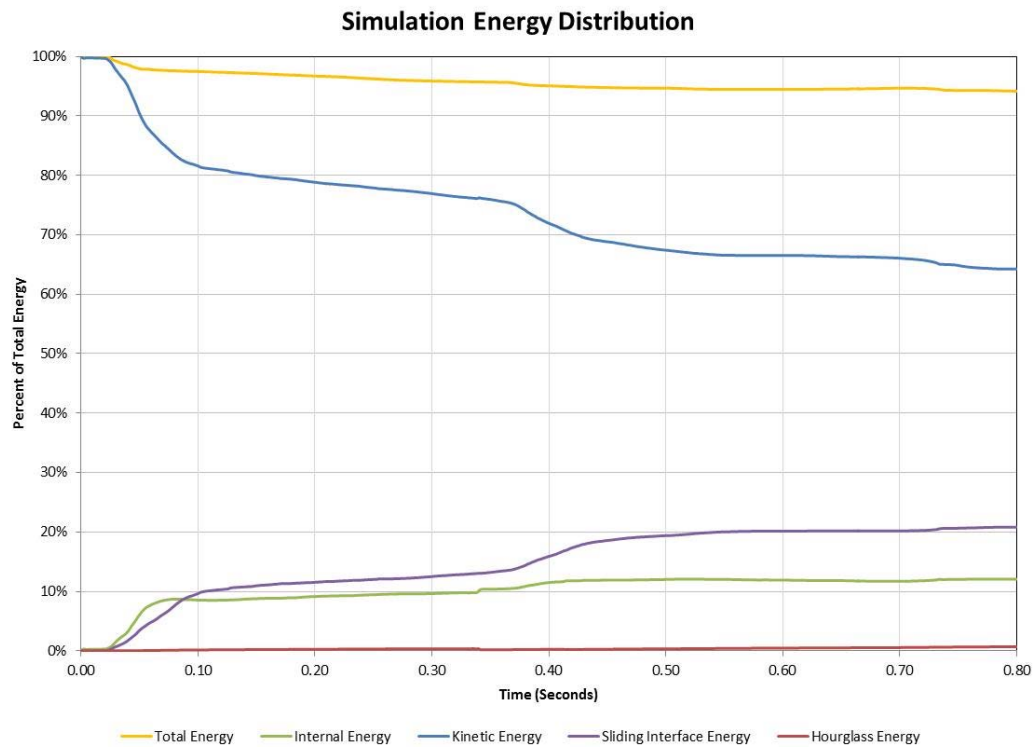


Figure 5.5: Energy Distribution Time History

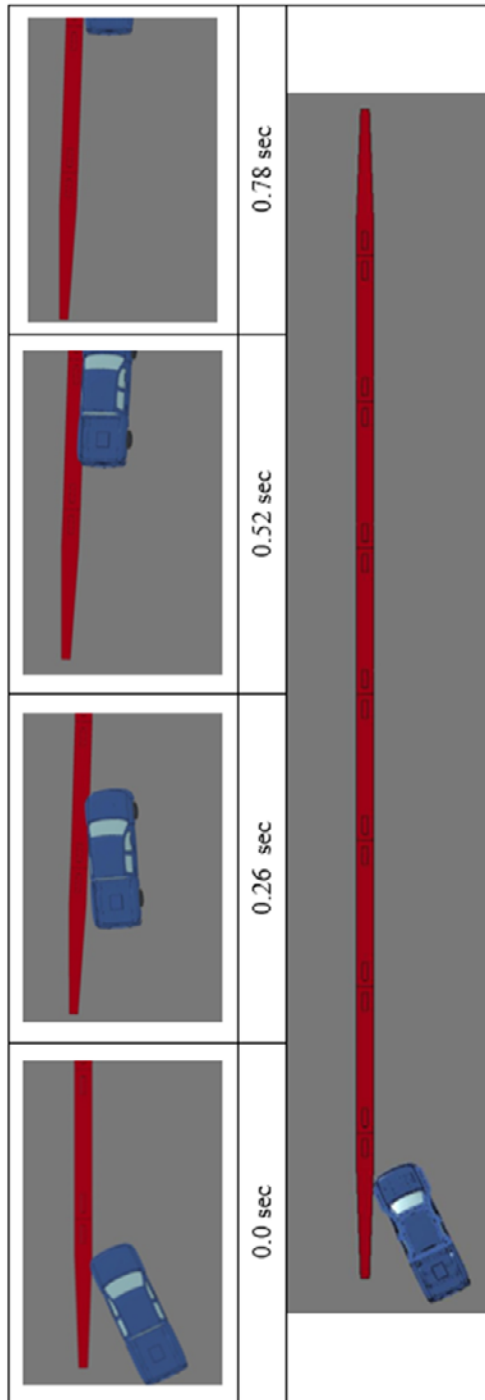
Occupant Risk and Vehicle Stability

Data acquired from the accelerometer, located at the vehicle center of gravity, were digitized for evaluation of occupant risk. In the longitudinal direction, the occupant impact velocity was 10.2 ft/s at 0.129 s, the highest 0.010-s occupant ridedown acceleration was 2.3 Gs from 0.385 to 0.395 s, and the maximum 0.050-s average acceleration was -5.5 Gs between 0.025 and 0.075 s. In the lateral direction, the occupant impact velocity was 14.1 ft/s at 0.0.129 s, the highest 0.010-s occupant ridedown acceleration was 4.9 Gs from 0.391 to 0.401 s, and the maximum 0.050-s average was 7.1 Gs between 0.029 and 0.07 s. Theoretical Head Impact Velocity (THIV) was 17.7 ft/s at 0.124 s; Post-Impact Head Decelerations (PHD) was 5.0 Gs between 0.391 and 0.401 s; and Acceleration Severity Index (ASI) was 0.97 between 0.056 and 0.106 s. All of which were within the preferred limits in accordance with MASH. These data and other pertinent information from the test are summarized in Figure 5.6. Vehicle angular displacements are presented in Figure B1.

After impact, the vehicle redirected and did not penetrate, underride, or override the installation. The maximum lateral deflection of the system was 28.8 inches and occurred at the nose of the end treatment. The vehicle remained upright and stable during the impact and after exiting the installation, with maximum roll and pitch angles of 14.9 degrees and 3.8 degrees, respectively.

Summary

This FEA supports the review and modifications presented in Chapter IV. The original system would function acceptably, but there are large lateral deflections. With the addition of the plate washer to the connection, lateral deflections only reach 28.8 inches. Thus, the FEA supports that the system should function within acceptable limits. Based on this FEA, the author proceeded with the full-scale crash test.



General Information		Impact Conditions		Vehicle Stability	
Test Agency	Texas A&M Transportation Institute (TTI)	Speed	4.0 mi/h	Maximum Yaw Angle	29.3 degrees
Test Standard Test No.	Simulation #1	Angle	25 degrees	Maximum Pitch Angle	-7.2 degrees
Date	N/A	Location/Orientation	79 inches upstream of splice	Maximum Roll Angle	-16.4 degrees
Test Article		Impact Severity		Vehicle Snagging	No
Type	Terminal	Occupant Risk Values		Vehicle Pocketing	No
Name	Non-pinned Low-Profile Barrier	Impact Velocity		Test Article Deflections	
Installation Length	160 ft	Longitudinal	10.2 ft/s	Dynamic	28.8 inches
Material or Key Elements	20 ft reinforced concrete	Lateral	-14.1 ft/s		
Test Vehicle		Ridedown Accelerations			
Type/Designation	2270P	Longitudinal	-2.3 G		
Make and Model	NCAC Chevrolet Silverado	Lateral	4.9 G		
Curb	5000 lb	THIV	17.7 ft/s		
Test Inertial	5000 lb	PHD	5.0 G		
Dummy	No Dummy	ASI	0.97		
Gross Static	500 lb	Max. 0.050-s Average			
		Longitudinal	-5.5 G		
		Lateral	7.1 G		
		Vertical	2.9 G		

Figure 5.6: Summary of Results for FEA Simulation

CHAPTER VI

FULL-SCALE CRASH TESTING

A full-scale crash test was conducted on the Low-Profile Portable Concrete Barrier (PCB) system, including the non-pinned Low-Profile PCB end treatment and Low-Profile PCB segment, to evaluate its performance relative to structural adequacy, occupant risk, and vehicle stability. This test was conducted at the Texas A&M Transportation Institute Proving Ground. This test involved a 2006 Dodge Ram 1500 pickup truck weighing 5,016 lb impacting the Low-Profile PCB system at a speed of 45 mi/h and angle of 25.3 degrees. The height to the lower and upper edge of the bumper was 15.25 inches and 28.00 inches, respectively. Figure 6.1 and 6.2 presents the 2006 Dodge Ram 1500 pickup truck used in the crash test. Table C1 and C2 in Appendix C provides additional dimensions and vehicle information. The test vehicle was towed into the Low-Profile PCB system using a steel cable guidance and reverse tow system. Just prior to impact of the test article, the vehicle was released causing it to be free-wheeling and unrestrained. The vehicle remained free-wheeling until it cleared the immediate test site area, at which point brakes were activated.



Figure 6.1: Vehicle/Installation Geometrics
(Beason et al 2013)



Figure 6.2: Vehicle Before Test
(Beason et al 2013)

TEST RESULTS

The vehicle was traveling at a speed of 45.0 mi/h when it impacted the non-pinned Low-Profile end treatment 78 inches upstream of the splice. The impact angle was 25.3 degrees. At approximately 0.013 s, the vehicle began to redirect, and at 0.036 s, the end of the terminal began to deflect towards the field side. The vehicle was traveling parallel with the barrier at 0.297 s, and the rear of the vehicle contacted the barrier at 0.348 s. As the vehicle continued forward, it left the view of the overhead high-speed camera making exit speed and angle unobtainable. However, judging from tire tracks, the vehicle exited the barrier at approximately 10 degrees, and came to rest 160 feet downstream of impact and 171 feet toward traffic lanes. Figure 6.3 depicts the test article and vehicle after completion of the test. Figure 6.4 presents a summary schematic of the crash test. Sequential photographs of the test are presented in Figure C1 and C2 of Appendix C (Beason et al 2013).



Figure 6.3: Installation and Vehicle Position After Test
(Beason et al 2013)

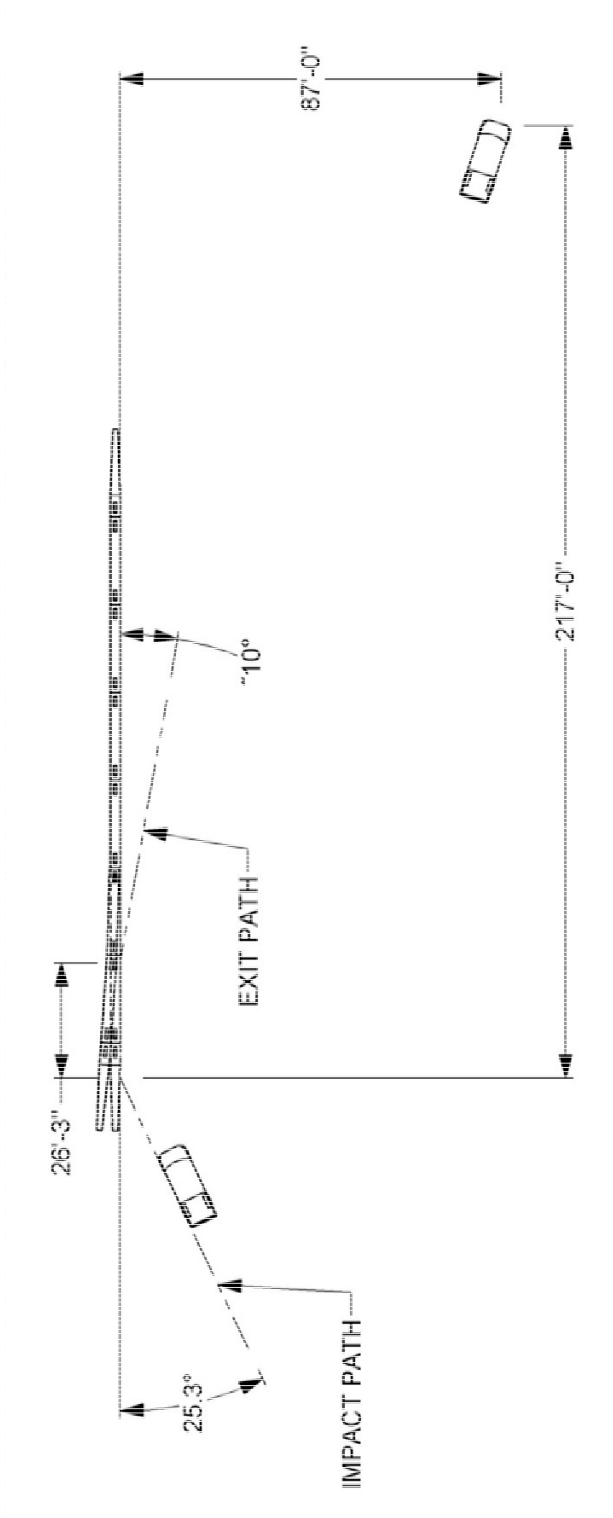


Figure 6.4: Crash Test Summary Schematic

The barrier received some damage, including concrete spalling along the impact area and on the field side at joint 2-3 which can be seen in figure 6.5. The damage did not expose any reinforcing steel and was not considered to significantly affect the structural integrity of the barrier system. The plate washers were deformed at joint 2-3. Figure 6.6 depicts the deformation found in the plate washer. Additionally, the threaded steel rods were bent slightly. The maximum lateral deflection of the barrier was 42.4 inches towards the field side at the nose of the end treatment. Deflections toward the field side were noticed at several downstream joints; Joint 1-2 deflected 25 inches, joint 2-3 deflected 9 inches, joint 3-4 deflected 2 inches and lastly joint 4-5 deflected 1 inch.

The vehicle suffered damage. The left lower control arm was deformed. The front bumper, left front fender, left front tire and wheel rim, left front and rear doors, left rear of the cab, left exterior bed, left rear front tire and wheel rim, and the rear bumper sustained damage. The vehicle suffered a maximum exterior crush of 14.0 inches at the left front corner of the bumper. No occupant compartment deformation occurred. Figure 6.7 shows the damage to the vehicle. Figure 6.8 shows the interior of the vehicle before and after impact. Details of the exterior crush and occupant compartment are presented in Table C3 and C4 of Appendix C.



Figure 6.5: Installation After Test
(Beason et al 2013)

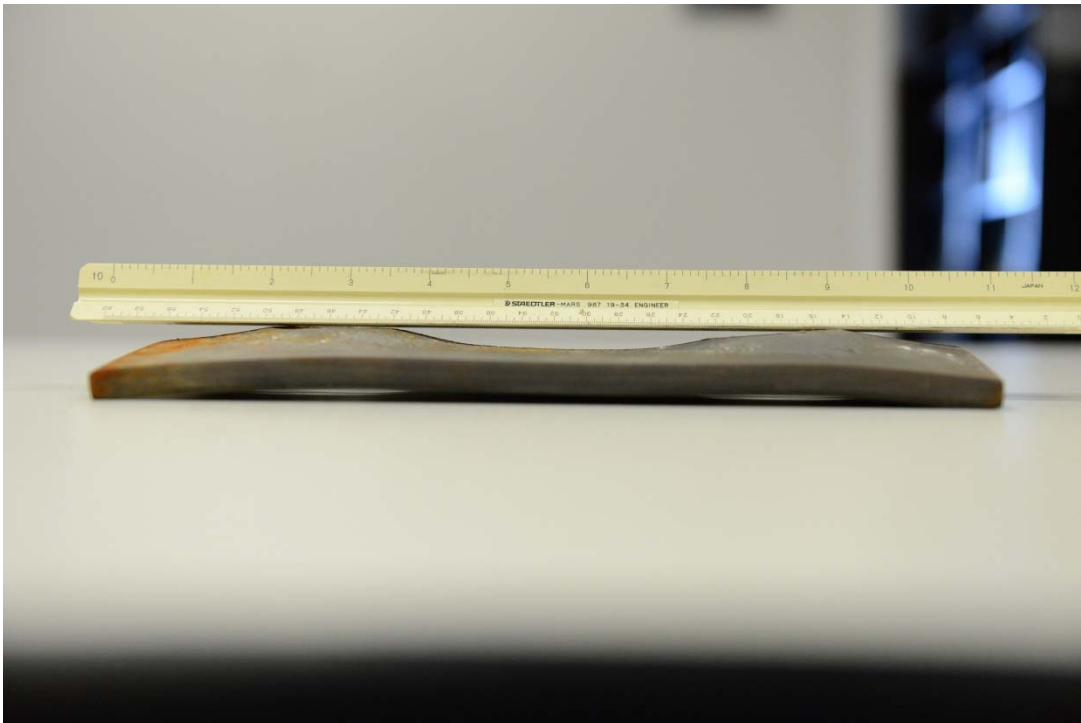


Figure 6.6: Joint 2-3 Plate Washer Deformation



Figure 6.7: Vehicle After Test
(Beason et al 2013)



Figure 6.8: Interior of Vehicle Before and After Test
(Beason et al 2013)

Occupant Risk and Vehicle Stability

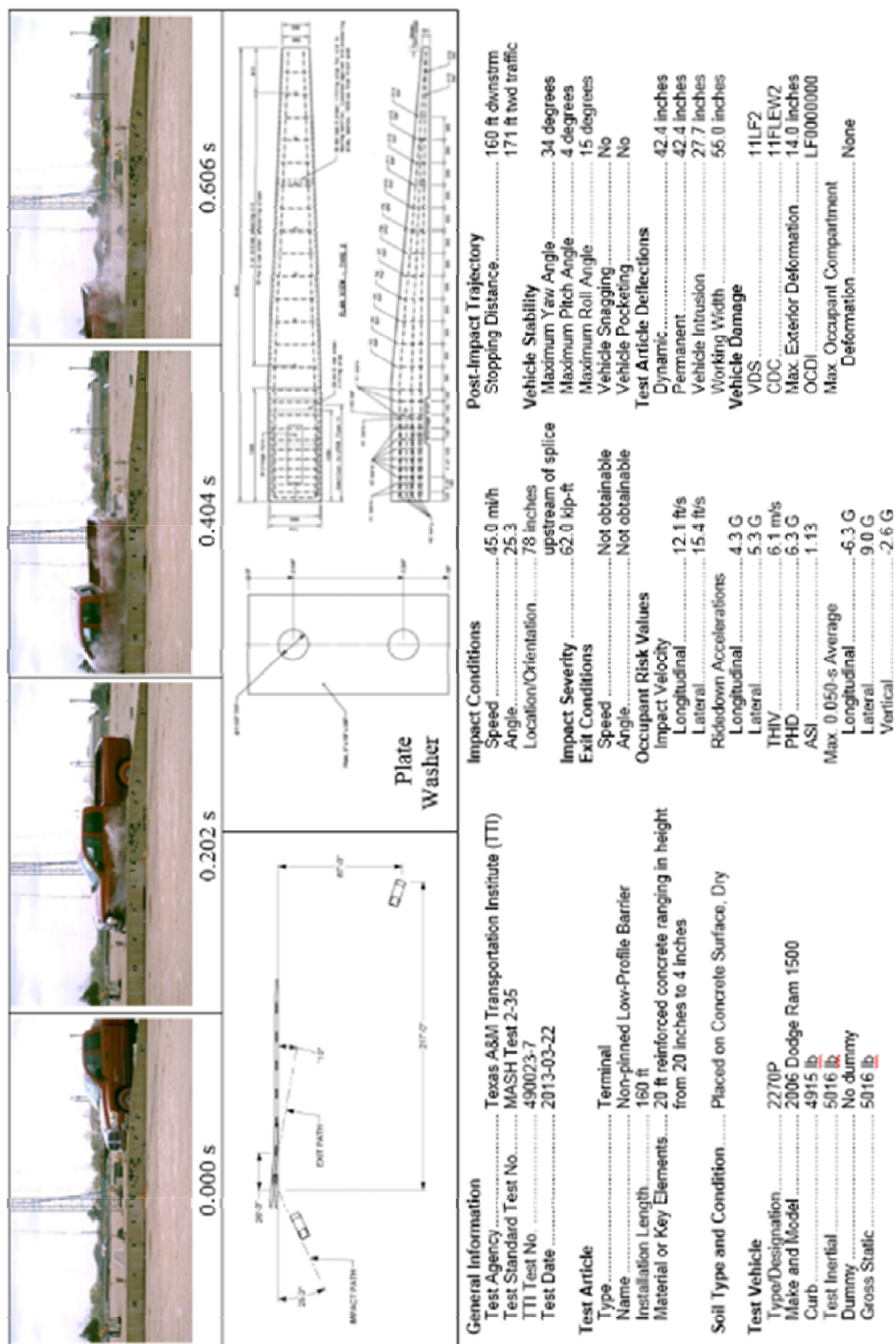
Data acquired from the accelerometer, located at the vehicle center of gravity, were digitized for evaluation of occupant risk. In the longitudinal direction, the occupant impact velocity was 12.1 ft/s at 0.121 s, the highest 0.010-s occupant ridedown acceleration was 4.3 Gs from 0.352 to 0.362 s, and the maximum 0.050-s average acceleration was -6.3 Gs between 0.034 and 0.084 s. In the lateral direction, the occupant impact velocity was 15.4 ft/s at 0.121 s, the highest 0.010-s occupant ridedown acceleration was 5.3 Gs from 0.323 to 0.333 s, and the maximum 0.050-s average was 9.0 Gs between 0.040 and 0.090 s. Theoretical Head Impact Velocity (THIV) was 20.0 ft/s at 0.116 s; Post-Impact Head Decelerations (PHD) was 6.3 Gs between 0.352 and 0.362 s; and Acceleration Severity Index (ASI) was 1.13 between 0.035 and 0.085 s. All of which were within the preferred limits in accordance with MASH. These data and other pertinent information from the test are summarized in Figure 6.9. Vehicle angular displacements and accelerations versus time traces are presented in Appendix C, Figures C4 through C7.

After impact, the vehicle redirected and did not penetrate, underride, or override the installation. The maximum lateral deflection of the system was 42.4 inches and occurred at the nose of the end treatment. There were no detached elements or debris to show potential for penetration of the occupant compartment or to present undue hazard to others in the area. There was no deformation or intrusion into the occupant compartment. The vehicle remained upright and stable during the impact and after exiting the installation, with maximum roll and pitch angles of 15 degrees and 4 degrees, respectively.

Summary

Full-scale crash tests results confirm the validity of the system's strength but raise questions about the FEA. The FEA resulted in a maximum lateral deflection of 28.8 inches while this full-scale crash test resulted in a maximum lateral deflection of 42.4 inches. There were no major issues with the original barrier system when the vertical pins are removed. The addition of the plate washer simply aides in the

connection threaded steel rod achieving full potential. Therefore, further analysis needs to be conducted to determine why a maximum lateral deflection difference of 13.6 inches exist between the FEA and full-scale crash test.



CHAPTER VII

FEA AND FULL-SCALE TESTING COMPARISON

The maximum lateral deflection of the Low-Profile PCB system in the full-scale crash test was 42.4 inches in the, but only 28.8 inches in the FEA. This raised questions about the confidence in the results from the FEA, which lead to further analysis and changes made to the FEA to more accurately simulate the full-scale test. It was discovered that the connection hole sizes in the field supplied barriers were not consistent with the design specifications. Therefore, the FE model was adjusted for the larger hole size. Additionally, it was noticed in the full-scale crash test that the end treatment lifted significantly while deflecting laterally. Thus, the friction factor in the FE model between the end treatment and the ground was cut down to 0.20.

This chapter provides a comparison of the results between full-scale crash test and the adjusted FE model simulation. The FE model replicated the full-scale crash test in terms of impact sequence of events, vehicle stability, and barrier system behavior. Table 7.1 to 7.3 illustrates the sequential comparison of the FEA simulation and full-scale crash test in an overhead view, rear view, and right angle view. Table 7.4 compares the occupant risk factors. These values are similar and, most importantly, within MASH limits. A comparison of the vehicle angular displacements can be seen in Table 7.5 or Figure 7.1. These displacements are slightly different. In order to determine orientation of the vehicle, angular displacements must be read in the following sequence: Yaw, Pitch, and Roll.

Table 7.1: Overhead View Sequential Comparison (Beason et al 2013)


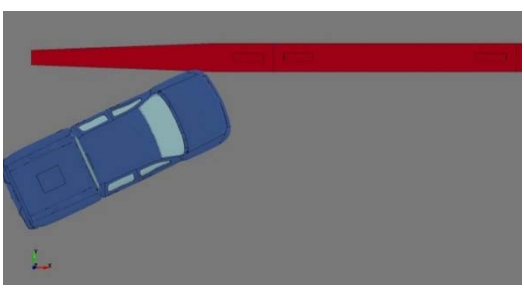

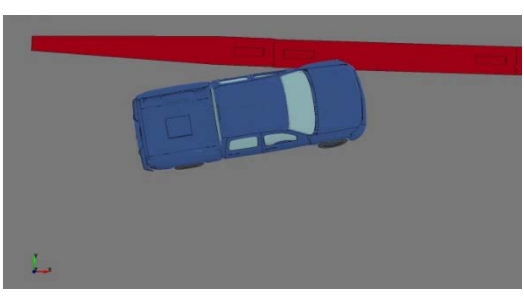

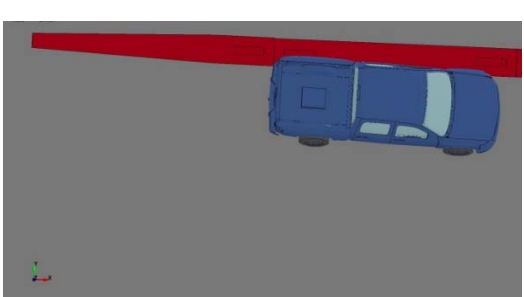

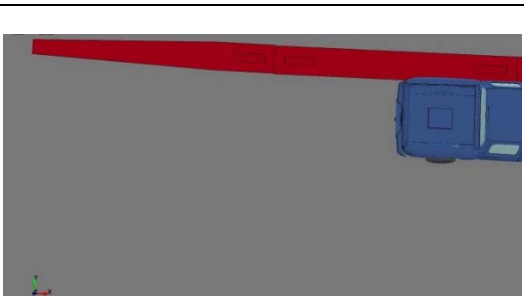
Time (sec)	Full-Scale Crash Test	FEA Simulation
0.000		
0.202		
0.404		
0.606		

Table 7.1: Continued


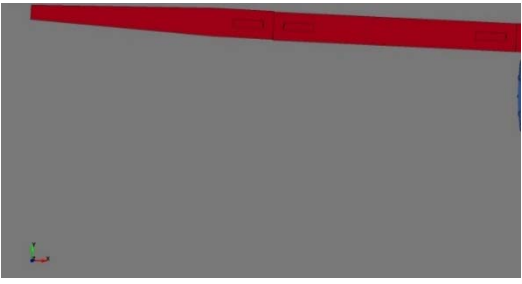
Time (sec)	Full-Scale Crash Test	FEA Simulation
0.808		
1.010	Vehicle Out of View	Vehicle Out of View
1.212	Vehicle Out of View	Vehicle Out of View
1.414	Vehicle Out of View	Vehicle Out of View

Table 7.2: Right Angle View Sequential Comparison (Beason et al 2013)


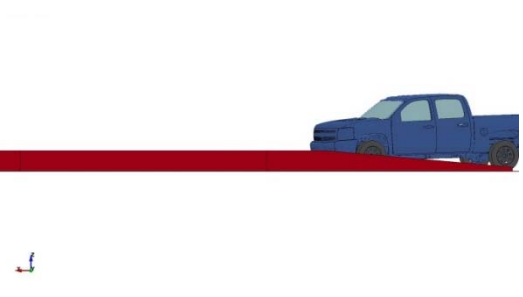

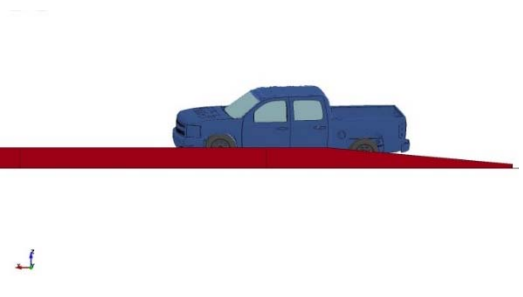

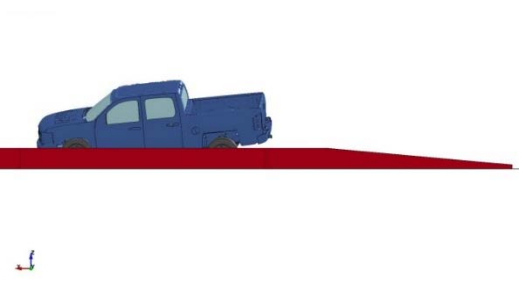

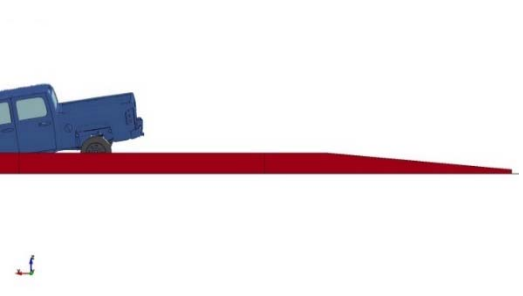
Time (sec)	Full-Scale Crash Test	FEA Simulation
0.000		
0.202		
0.404		
0.606		

Table 7.2: Continued



Time (sec)	Full-Scale Crash Test	FEA Simulation
0.808		
1.010	Vehicle Out of View	Vehicle Out of View
1.212	Vehicle Out of View	Vehicle Out of View
1.414	Vehicle Out of View	Vehicle Out of View

Table 7.3: Rear View Sequential Comparison (Beason et al 2013)


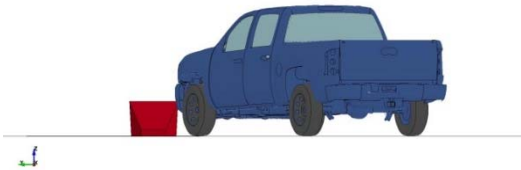

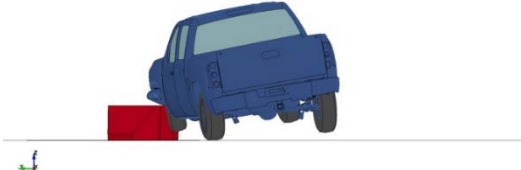

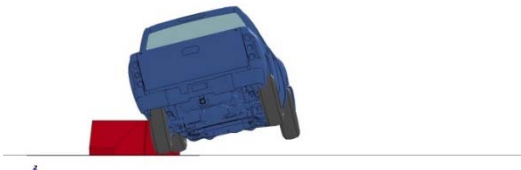

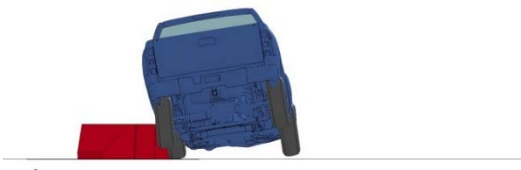

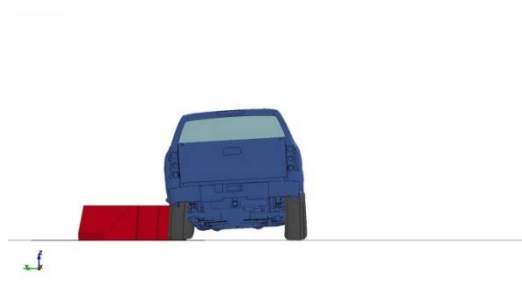

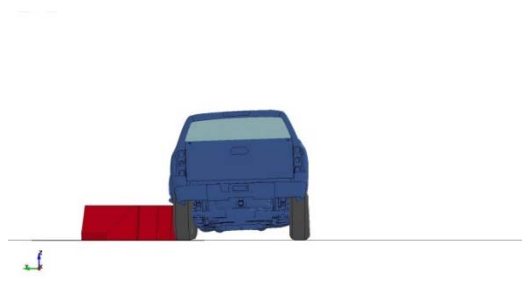
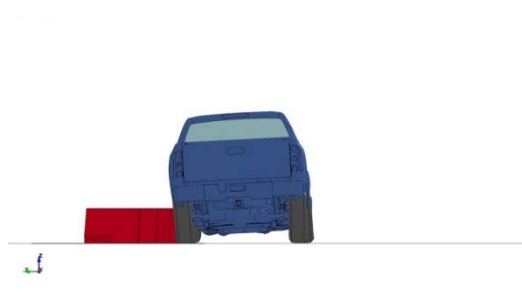

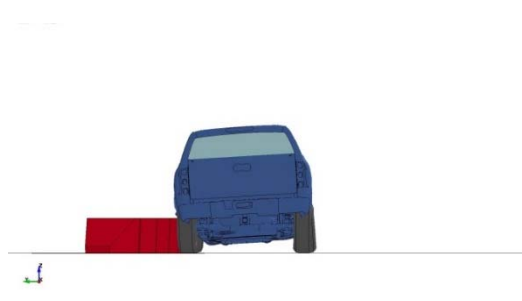
Time (sec)	Full-Scale Crash Test	FEA Simulation
0.000		
0.202		
0.404		
0.606		

Table 7.3: Continued

Time (sec)	Full-Scale Crash Test	FEA Simulation
0.808		
1.010		
1.212		
1.414		

Yaw, Pitch, and Roll Angle Comparison

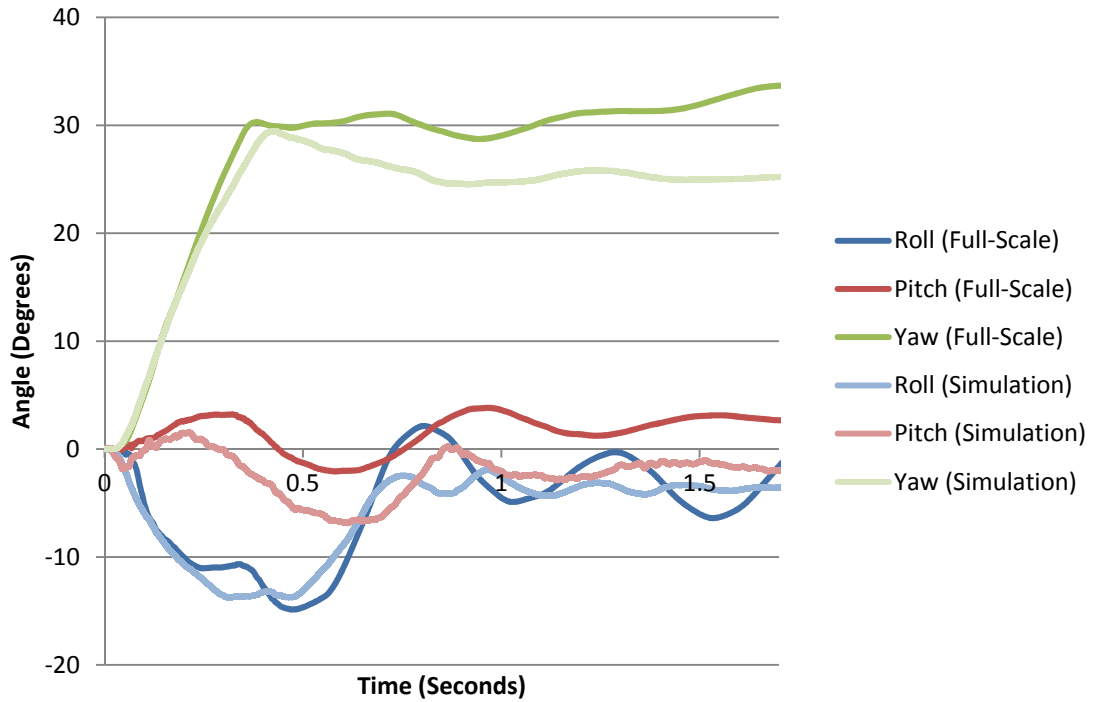


Figure 7.1: Vehicle Angular Displacement Comparison

Table 7.4: Yaw, Pitch, and Roll Maximum Value Comparison

Angles	Full-Scale Crash Test	FEA Simulation
Roll (degrees)	-14.9	-13.8
Pitch (degrees)	3.8	-6.9
Yaw (degrees)	33.7	29.5

Table 7.5: Occupant Risk Factor Comparison

Occupant Risk Factors	Full-Scale Crash Test	FEA Simulation
Impact Velocity (ft/s)		
x-direction	12.14	10.17
y-direction	-15.42	-13.78
Ridedown Acceleration (g's)		
x-direction	-14.12	-8.86
y-direction	17.39	17.72
THIV (ft/s)		
	20.01	17.39
PHD (g's)		
	6.3	5.4
ASI		
	1.20	0.94

The comparison figures and tables above illustrate that the vehicle behaved similarly in both the full-scale crash test and the adjusted FEA. After the FEA was adjusted for larger connection holes and the static frictional coefficient was cut to 0.20 on the end treatment, the maximum lateral deflection was 39.5 inches. When compared to the 42.4 inch deflection found in the full-scale crash test, the FEA deflection was within 7%. It is believed, this slight discrepancy is due to the assumption that the barrier in the FEA is assumed to be rigid and therefore does not model the spalling that existed in the full-scale crash test.

With the adjustment to the FE model yielding results nearly identical to those of full-scale crash test, it is important for fabricators to pay close attention to the details of

the design specifications. When the connection holes were modeled as 1.5 inch diameter holes, the maximum lateral deflection was 28.8inches. That deflection increased to 39.5 inches when the connection holes were modeled as 2 inch diameter holes, as found in the field supplied barriers.

CHAPTER VIII

CONCLUSION

Through the use of sound engineering judgment and approximate strength analyses of the original Low-Profile PCB design, the author determined the system would most likely function acceptably. However, the lateral displacement would be too large to allow the barrier to be deployed next to a drop off. In order to control lateral displacement, the rigidity of the connection needed to be increased. Therefore, a plate washer was added to the connection insuring the connection threaded steel rod would be able to reach its full capacity.

The system recommended has minor changes which were analyzed with FEA and a full-scale crash test. The FEA was more difficult as the barrier system was free standing without positive attachment, there were large deflections, and the material was non-linear. Nevertheless, the FEA model worked reasonably well in modeling the system.

The non-pinned Low-Profile PCB system has passed the MASH test 2-35, test for strength, in both a full-scale crash test and FEA. While this does not replace the original barrier, it does provide another option for use of the Low-Profile PCB in situations where sufficient room for deflection outside of the length of need exists. If this room does not exist, the barrier must be pinned.

REFERENCES

- American Association of State Highway and Transportation Officials (AASHTO). (2009). "Manual for Assessing Safety Hardware." AASHTO, Washington, D.C.
- Beason, W.L. (1992). "Development of an End Treatment For a Low-Profile Portable Concrete Barrier." *Final Report No. 990-4F*, Texas Transportation Institute, College Station, TX.
- Beason, W.L., Menges, W.L., and Ivey, D.L. (1998). "Compliance Testing of an End Treatment For a Low-Profile Portable Concrete Barrier." *Final Report No. 1403-S*, Texas Transportation Institute, College Station, TX.
- Beason, W.L., Brackin, M.S., Bligh, R.P., and Menges, W.L. (2013). "Development and Testing of a Non-Pinned Low-Profile End Treatment." *Final Report No. 9-1002-12-7*, Texas A&M Transportation Institute, College Station, TX.
- Guidry, T.R., and Beason, W.L. (1991). "Development of a Low-Profile Portable Concrete Barrier." *Final Report No. 1949-2*, Texas Transportation Institute, College Station, TX.
- Hallquist, J.O. (2012). "LS-DYNA Keyword User's Manual." Version 971 R6.1.0, Livermore Software and Technology Corporation, Livermore CA.
- Kozel, S.M. (1997). "New Jersey Median Barrier History." Roads to the Future, <http://www.roadstothefuture.com/Jersey_Barrier.html>
- Marzougui, D. et al (2001). "Evaluation of Portable Concrete Barriers Using Finite Element Simulation." *Journal of the Transportation Research Board*, Transportation Research Board, 1720.
- McDevitt, C.F. (2000). "Basics of Concrete Barriers." *Public Roads*, 63(5), 10-14.
- Michie, J.D. (1980) "Recommended Procedures for the Safety Performance Evaluation of Highway Appurtenances." *NCHRP Report 230*, Transportation Research Board, Washington, D.C.
- Oden, J.T, et al. (2006) "Revolutionizing Engineering Science through Simulation." *Simulation-Based Engineering Science*, National Science Foundation.
- Reid, J.D. (2004). "LS-DYNA Simulation Influence on Roadside Hardware." *Journal of the Transportation Research Board*, Transportation Research Board, 1890, 34-41.

Ross, H.E. Jr., Sicking, D.L., Zimmer, R.A., Michie, J.D.(1993) "Recommended Procedures for the Safety Performance Evaluation of Highway Features." *NCHRP Report 350*, Transportation Research Board, Washington, D.C.

APPENDIX A
LOW-PROFILE PORTABLE CONCRETE BARRIER DETAILS

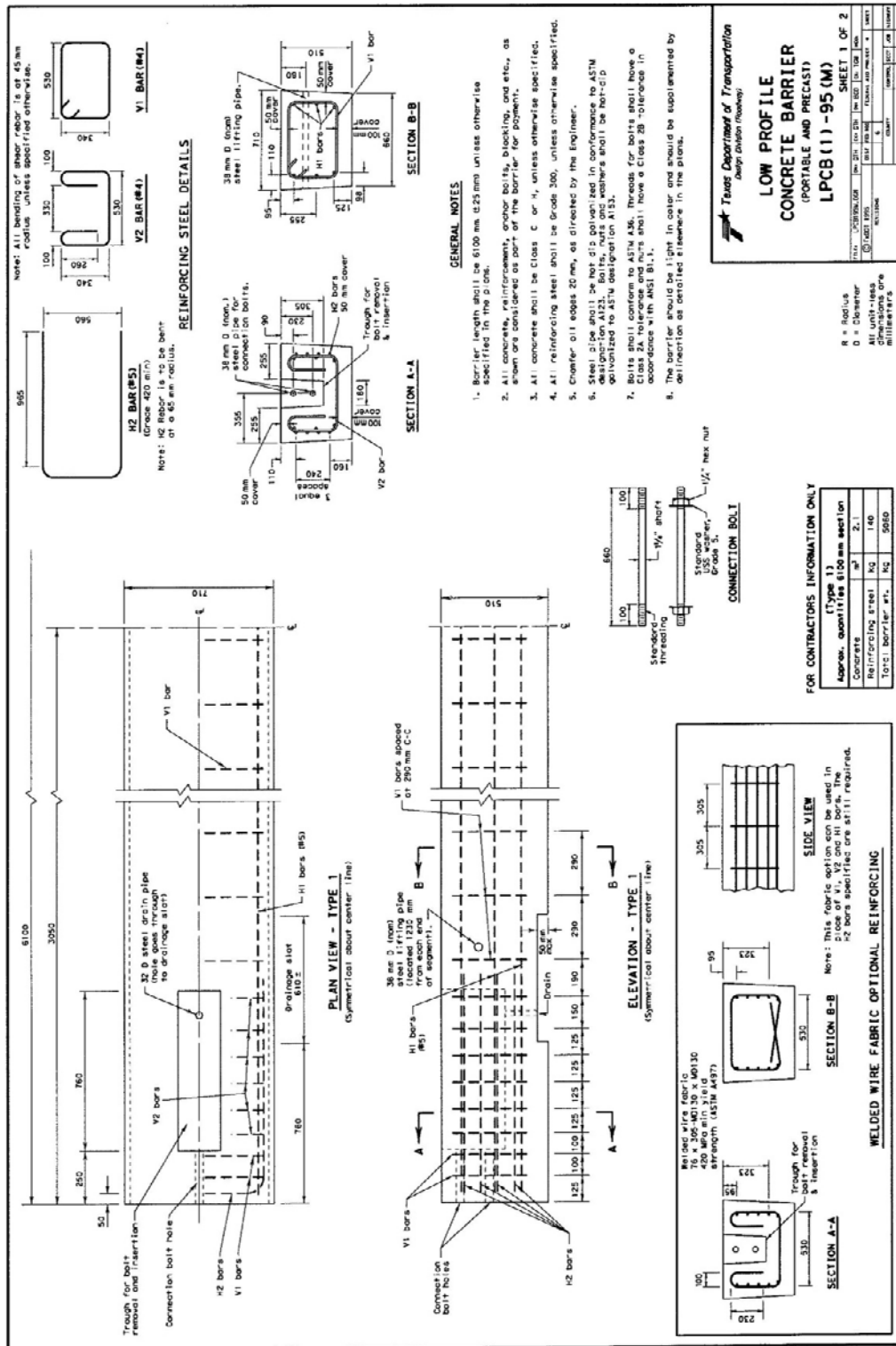
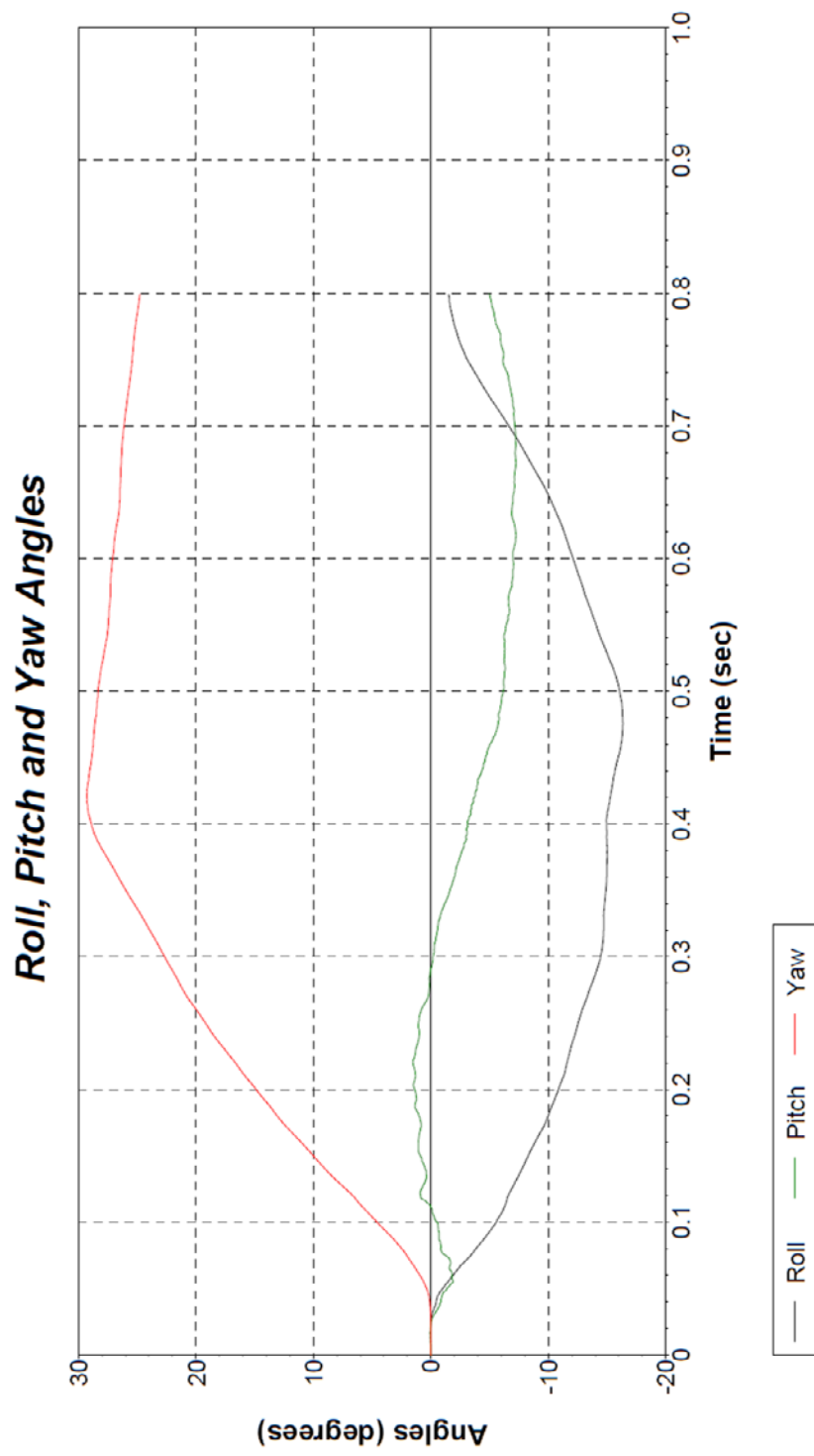


Figure A1: Low-Profile PCB Segment Details

APPENDIX B
FINITE ELEMENT ANALYSIS ANGULAR DISPLACEMENT DATA



Axes are vehicle-fixed.
Sequence for determining
orientation:

1. Yaw.
2. Pitch.
3. Roll.

Figure B1: Vehicle Angular Displacements

APPENDIX C
FULL-SCALE CRASH TEST INFORMATION

Table C1: Vehicle Properties (Beason et al 2013)

Date: 2013-03-22 Test No.: 490023-7 VIN No.: 1D7HA18No65693242
 Year: 2006 Make: Dodge Model: Ram 1500
 Tire Size: P265/70R17 Tire Inflation Pressure: 35 psi
 Tread Type: Highway Odometer: 124208

Note any damage to the vehicle prior to test: _____

• Denotes accelerometer location.

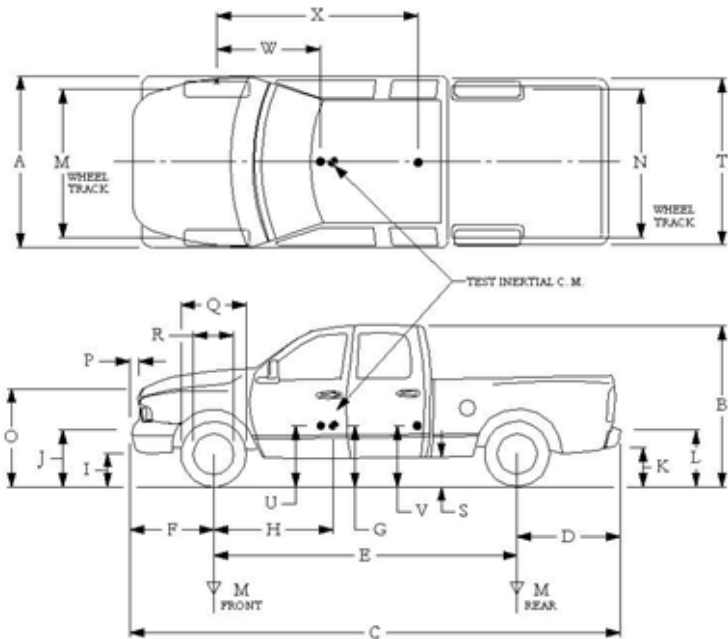
NOTES: _____

Engine Type: V8
 Engine CID: 4.7 liter

Transmission Type:
☒ Auto or ☐ Manual
☐ FWD ☒ RWD ☐ 4WD

Optional Equipment: _____

Dummy Data:
 Type: None
 Mass: _____
 Seat Position: _____



Geometry: inches

A	78.25	F	36.00	K	21.50	P	2.88	U	28.50
B	75.50	G	28.00	L	30.25	Q	30.50	V	30.50
C	223.75	H	62.52	M	68.50	R	18.38	W	61.50
D	47.25	I	15.25	N	68.00	S	16.00	X	80.00
E	140.50	J	28.00	O	45.50	T	77.50		
Wheel Center Height Front	14.75	Wheel Well Clearance (Front)	6.00	Bottom Frame Height - Front	11.75				
Wheel Center Height Rear	14.75	Wheel Well Clearance (Rear)	10.25	Bottom Frame Height - Rear	26.00				

RANGE LIMIT: A=78 ±2 inches; C=237 ±13 inches; E=148 ±12 inches; F=39 ±3 inches; G = > 28 inches; H = 63 ±4 inches; O=43 ±4 inches; M+N/2=67 ±1.5 inches

GVWR Ratings:	Mass: lb	Curb	Test Inertial	Gross Static
Front	3700	<u>M_{front}</u>	2862	2784
Back	3900	<u>M_{rear}</u>	2053	2232
Total	6700	<u>M_{Total}</u>	4915	5016

(Allowable Range for TIM and GSM = 5000 lb ±110 lb)

Mass Distribution:

lb LF: 1401 RF: 1383 LR: 1109 RR: 1173

Table C2: Measurement of Vehicle CG (Beason et al 2013)

Date: 2013-03-22 Test No.: 490023-7 VIN: 1D7HA18No65693242
 Year: 2006 Make: Dodge Model: Ram 1500
 Body Style: Quad Cab Mileage: 124208
 Engine: 4.7 liter V8 Transmission: Automatic
 Fuel Level: Empty Ballast: 214 lb (440 lb max)
 Tire Pressure: Front: 35 psi Rear: 35 psi Size: P265/70R17

Measured Vehicle Weights: (lb)					
LF:	1401	RF:	1383	Front Axle:	2784
LR:	1109	RR:	1123	Rear Axle:	2232
Left:	2510	Right:	2506	Total:	5016
5000 ±110 lb allowed					
Wheel Base:	140.5 inches	Track: F:	68.5 inches	R:	68 in
148 ±12 inches allowed		Track = (F+R)/2 = 67 ±1.5 inches allowed			
Center of Gravity, SAE J874 Suspension Method					
X:	62.52 inches	Rear of Front Axle (63 ±4 inches allowed)			
Y:	-0.03 inches	Left - Right + of Vehicle Centerline			
Z:	28 inches	Above Ground (minumum 28.0 inches allowed)			

Hood Height: 44.50 inches Front Bumper Height: 28.00 inches
 43 ±4 inches allowed

Front Overhang: 36.00 inches Rear Bumper Height: 30.25 inches
 39 ±3 inches allowed

Overall Length: 223.75 inches
 237 ±13 inches allowed

Table C3: Exterior Crush Measurements (Beason et al 2013)

Date: 2013-03-22 Test No.: 490023-7 VIN No.: 1D7HA18No65693242
 Year: 2006 Make: Dodge Model: Ram 1500

VEHICLE CRUSH MEASUREMENT SHEET¹

Complete When Applicable	
End Damage	Side Damage
Undeformed end width _____	Bowing: B1 _____ X1 _____
Corner shift: A1 _____	B2 _____ X2 _____
A2 _____	
End shift at frame (CDC)	Bowing constant
(check one)	$\frac{X1 + X2}{2} = \underline{\hspace{2cm}}$
< 4 inches _____	
≥ 4 inches _____	

Note: Measure C₁ to C₆ from Driver to Passenger side in Front or Rear impacts – Rear to Front in Side Impacts.

Specific Impact Number	Plane* of C-Measurements	Direct Damage		Field L**	C ₁	C ₂	C ₃	C ₄	C ₅	C ₆	±D
		Width** (CDC)	Max*** Crush								
1	Front plane at bumper ht	17	14	24	14	12	8	3	1	0	-17.5
2	Side plane at bumper ht	17	12	48	0	1/2	---	---	10	12	+76
	Measurements recorded										
	in inches										

¹Table taken from National Accident Sampling System (NASS).

*Identify the plane at which the C-measurements are taken (e.g., at bumper, above bumper, at sill, above sill, at beltline, etc.) or label adjustments (e.g., free space).

Free space value is defined as the distance between the baseline and the original body contour taken at the individual C locations. This may include the following: bumper lead, bumper taper, side protrusion, side taper, etc. Record the value for each C-measurement and maximum crush.

**Measure and document on the vehicle diagram the beginning or end of the direct damage width and field L (e.g., side damage with respect to undamaged axle).

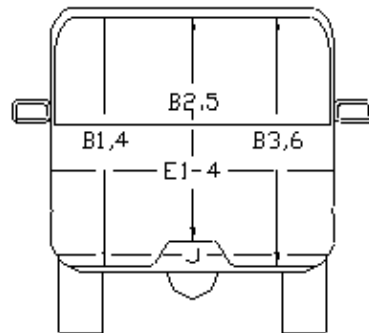
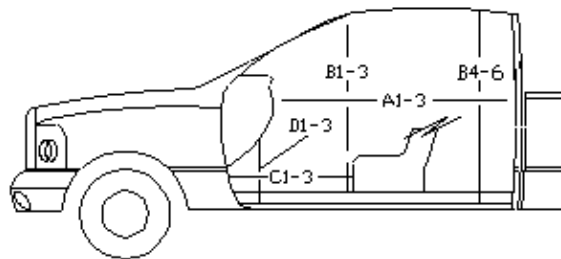
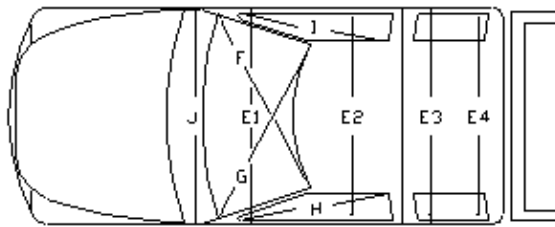
***Measure and document on the vehicle diagram the location of the maximum crush.

Note: Use as many lines/columns as necessary to describe each damage profile.

Table C4: Occupant Compartment Measurements (Beason et al 2013)

Date: 2013-03-22 Test No.: 490023-7 VIN No.: 1D7HA18No65693242

Year: 2006 Make: Dodge Model: Ram 1500



OCCUPANT COMPARTMENT DEFORMATION MEASUREMENT

	Before (inches)	After (inches)
A1	65.00	65.00
A2	64.50	64.50
A3	65.25	65.25
B1	45.25	45.25
B2	39.50	39.50
B3	45.25	45.25
B4	42.00	42.00
B5	45.00	45.00
B6	42.00	42.00
C1	30.00	30.00
C2	----	----
C3	27.00	27.00
D1	12.75	12.75
D2	----	----
D3	11.50	11.50
E1	62.75	62.75
E2	64.25	64.25
E3	64.00	64.00
E4	64.50	64.50
F	60.00	60.00
G	60.00	60.00
H	39.00	39.00
I	39.00	39.00
J*	62.25	62.25

*Lateral area across the cab from
driver's side kickpanel to passenger's side kickpanel.









Overhead View	Time (secs)	Right Angle View
	0.000	
	0.202	
	0.404	
	0.606	

Figure C1: Sequential Photographs (Overhead and Right Angle Views)
(Beason et al 2013)



Overhead View	Time (secs)	Right Angle View
	0.808	
Vehicle out of view	1.010	Vehicle out of view
Vehicle out of view	1.212	Vehicle out of view
Vehicle out of view	1.414	Vehicle out of view

Figure C1: Continued
(Beason et al 2013)

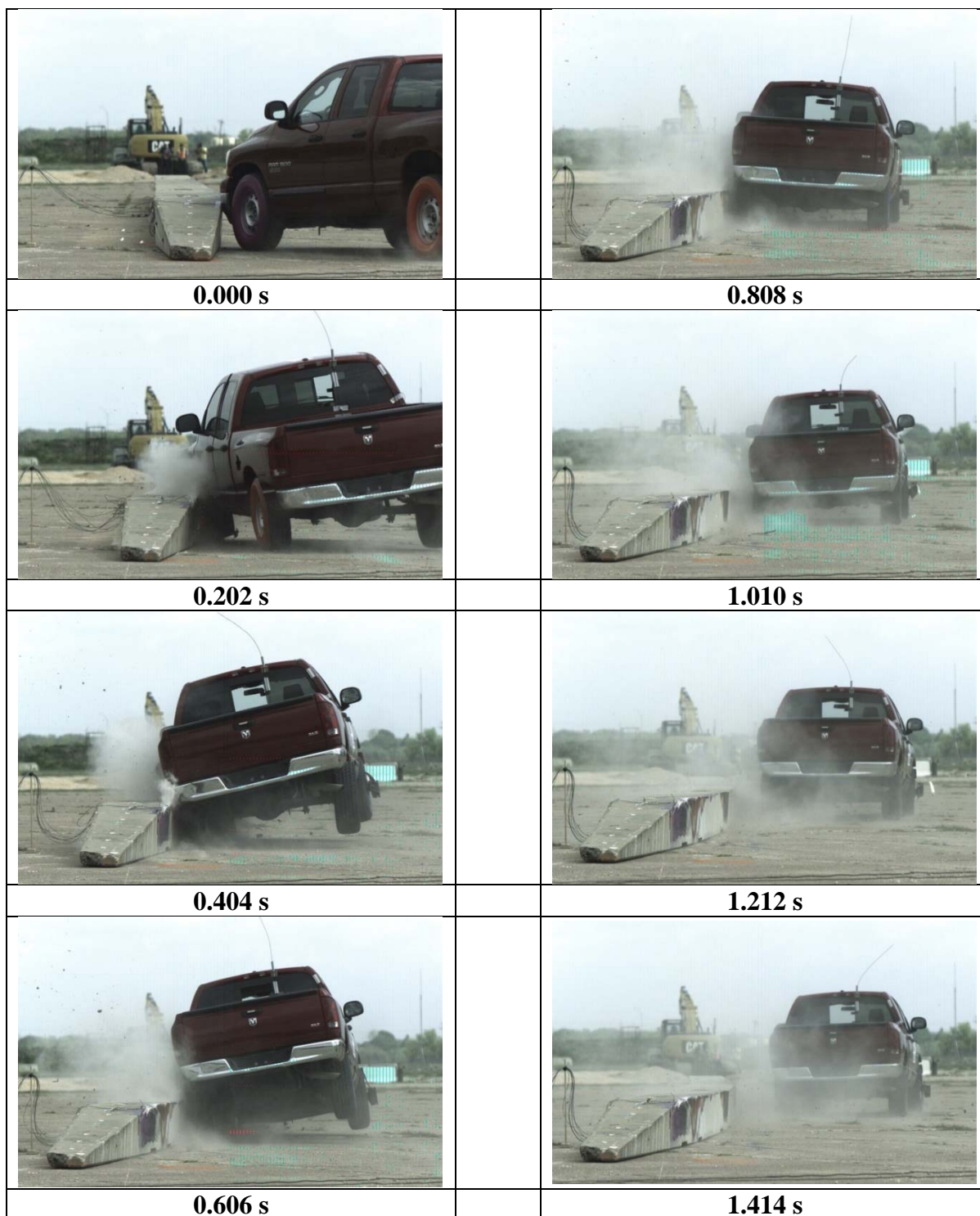


Figure C2: Sequential Photographs (Rear View)
(Beason et al 2013)

Roll, Pitch, and Yaw Angles

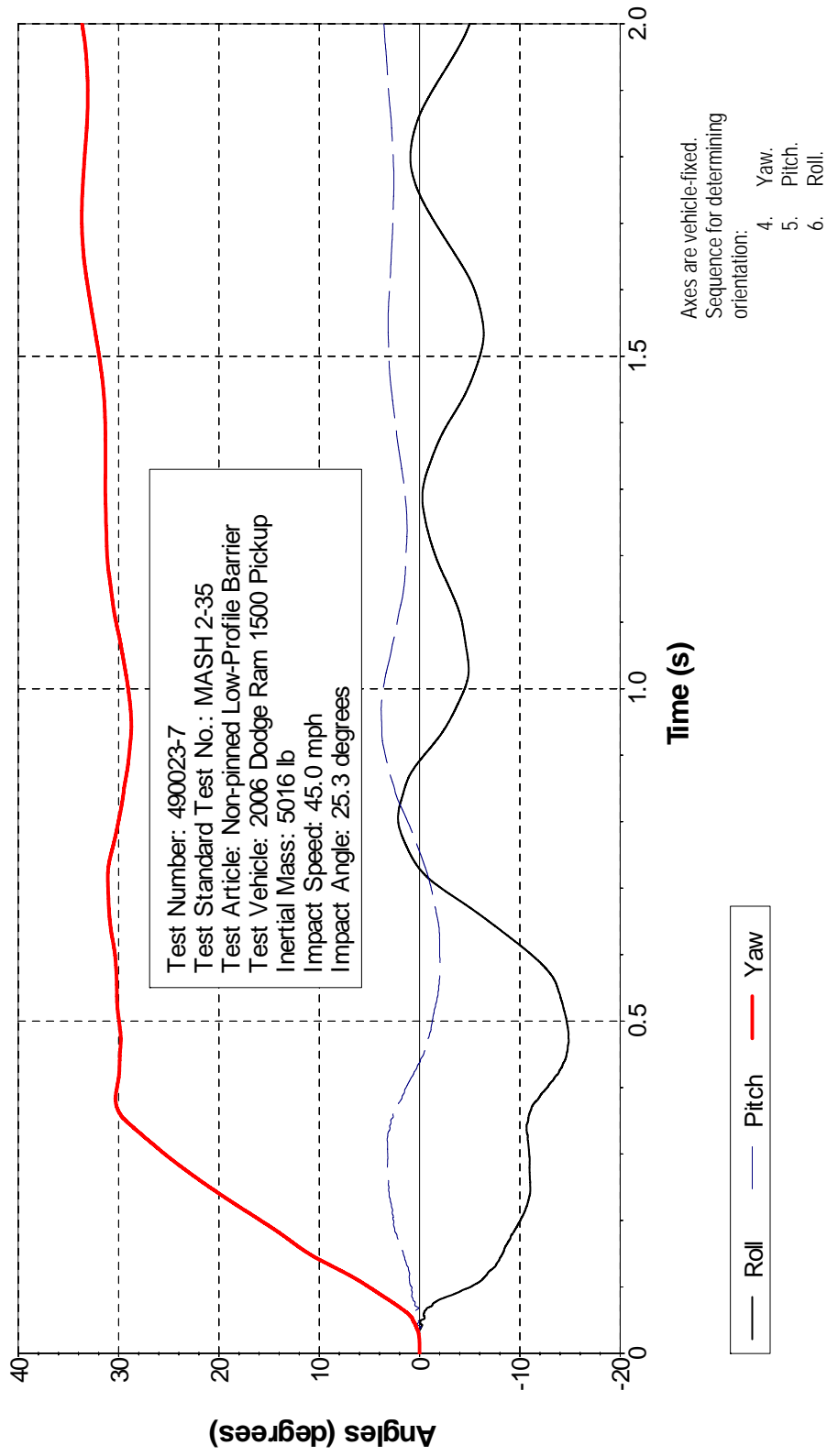


Figure C3: Vehicle Angular Displacements
 (Beason et al 2013)

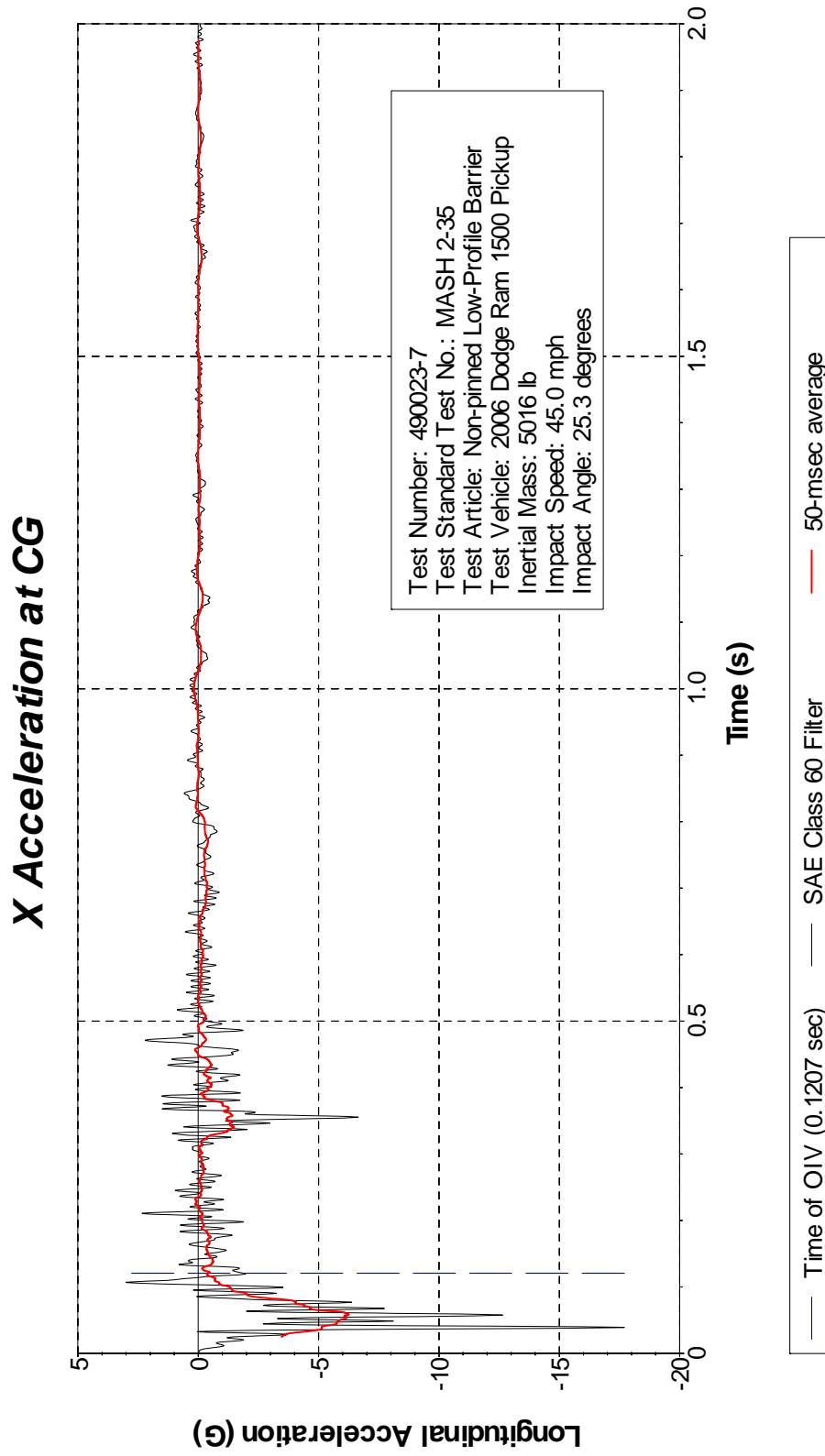


Figure C4: Vehicle Longitudinal Accelerometer Trace
 (Accelerometer Located at Center of Gravity)
 (Beason et al 2013)

Y Acceleration at CG

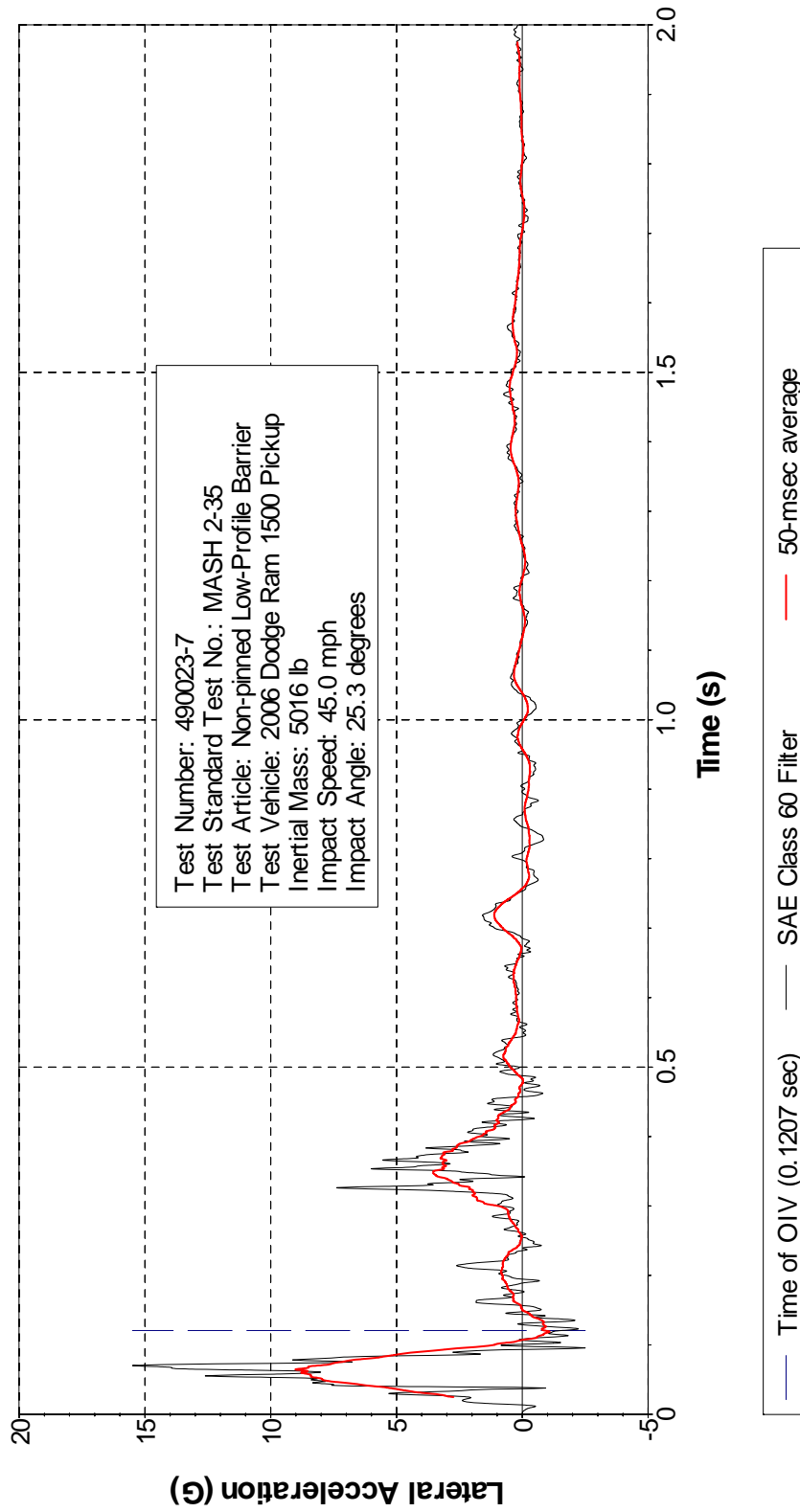


Figure C5: Vehicle Lateral Accelerometer Trace
 (Accelerometer Located at Center of Gravity)
 (Beason et al 2013)

Z Acceleration at CG

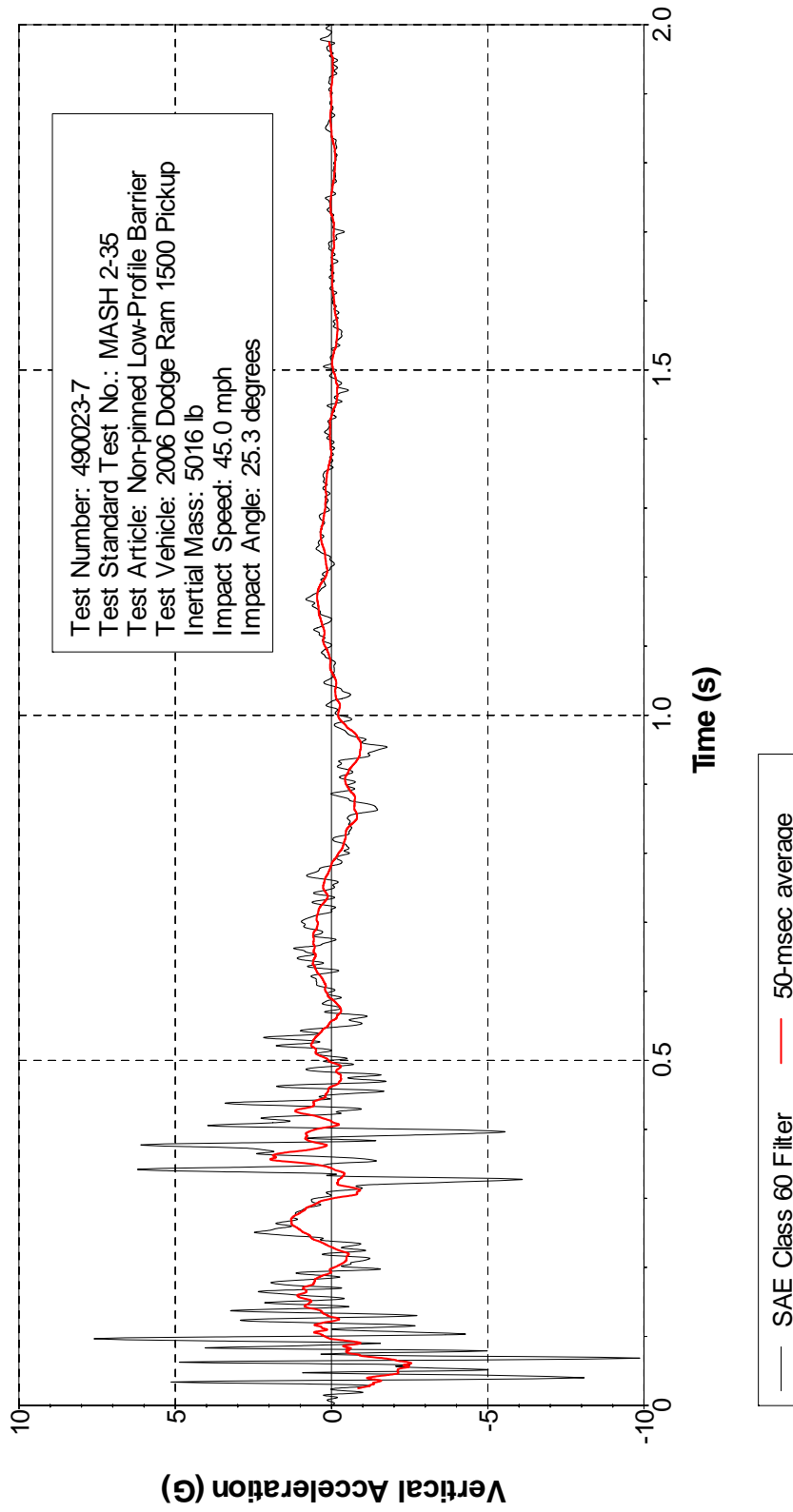


Figure C6: Vehicle Vertical Accelerometer Trace
(Accelerometer Located at the Center of Gravity)
(Beason et al 2013)